THESIS APPROVAL

GRADUATE SCHOOL, KASETSART UNIVERSITY

Master of Engineering (Chemical Engineering)

DEGREE

Chemical Engineering	Chemical Engineering
FIELD	**DEPARTMENT**

TITLE: Molecular Dynamics Simulation of Ion Conduction in Chitosan Membrane for PEM Fuel Cell

NAME: Ms. Suwalee Martkumchan

THIS THESIS HAS BEEN ACCEPTED BY

THESIS ADVISOR

(Associate Professor Thongchai Srinophakun, Ph.D.)

THESIS CO-ADVISOR

(Assistant Professor Manop Charoenchaitrakool, Ph.D.)

DEPARTMENT HEAD

(Associate Professor Phungphai Phanawadee, D.Sc.)

APPROVED BY THE GRADUATE SCHOOL ON _____

DEAN

(Associate Professor Gunjana Theeragool, D.Agr.)

THESIS

MOLECULAR DYNAMICS SIMULATION OF ION CONDUCTION IN CHITOSAN MEMBRANE FOR PEM FUEL CELL

SUWALEE MARTKUMCHAN

A Thesis Submitted in Partial Fulfillment of
the Requirements for the Degree of
Master of Engineering (Chemical Engineering)
Graduate School, Kasetsart University
2009

Suwalee Martkumchan 2009: Molecular Dynamics Simulation of Ion Conduction in Chitosan Membrane for PEM Fuel Cell. Master of Engineering (Chemical Engineering), Major Field: Chemical Engineering, Department of Chemical Enigineering. Thesis Advisor: Associate Professor Thongchai Srinophakun, Ph.D. 81 pages.

The propose of this research was to study the ion conductivity mechanism of chitosan membrane at the molecular level. Chitosan materials were formulated by molecular dynamics simulation named Materials Studio 4.3 using COMPASS force field. The systems contained chitosan, hydronium ions and various amounts of water, 10, 20, 30 and 40 wt% of water. The molecular dynamics simulation was used to estimate the diffusion coefficient, the ion conductivity and the coordinations between particles. The system containing 40 % of water by weight was suitable as a conducting material, which had an ion conductivity value of 10^{-2} S/cm. The results were compared with reference reported experimental data. Such material was studied in the temperature range of 298 – 360 K. The resulting conductivity followed Arrhenius behavior. Chitosan 70, 80 and 90 degree of deacetylation were studied at constant 40 % of water by weight. As a result, the ion conductivities were similar to the 40 % of water system. The coordination was studied to evaluate the location of particles in the system to understand the transport mechanism of the ions. Conductivity was appropriate in the systems in which the eigen ion and water clusters formed.

_____ _____ ___/___/___

Student's signature Thesis Advisor's signature

ACKNOWLADGEMENT

I would like to gratefully thank and I am deeply indebted to Assoc. Prof. Dr. Thongchai Srinophakun my thesis advisor for guidance and encouragement throughout the course of this work. He has taken care of me in every step in this work. I would like to express my appreciation to him for spending time and valuable suggestion for completely writing of thesis. Respective thanks go to my major committees, Assoc. Prof. Dr. Phungphai Phanawadee, Asst. Prof, Dr. Manop Charoenchaitrakool and graduate school representative, Dr. Patcharin Worathanakul for their great comments and suggestions.

This thesis was supported by Center of Excellence for Petroleum, Petrochemicals and Advanced Materials**.** I would like to thank the Accelrys Software Inc., NANOTEC and ThaiGrid center for the support Materials Studio sorfware. I would like to thank for Assoc. Prof. Dr. Supa Hannhongbua and Dr. Songwut Suramitr, who suggest me to use the software.

Oftentimes, I have difficulty in this work. My friends, G-5 stand together all the time. I would like to thank them for encouragement and helpful time.

I am especially appreciated my parents, my sister and brothers for their continue support and heartfelt love during my life.

Suwalee Martkumchan

April 2009

TABLE OF CONTENTS

Page

LIST OF TABLES

LIST OF TABLES (Continued)

LIST OF FIGURES

LIST OF FIGURES (Continued)

LIST OF FIGURES (Continued)

LIST OF ABBREVIATIONS

BLYP	=	Beck-Lee-Yang-Parr function
COMPASS	=	Condense phase optimized molecular potentials for atomistic simulation studies
D	=	Diffusion coefficient (m^2/s)
DDA	=	Degree of deacetylation
DFT	=	Density functional theory
EIS	=	Electrochemicals impedance spectroscopy
fs	=	Famto second (10^{-15} s)
HF	=	Hatree-Fock
k	=	Boltzman's constant
MC	=	Monte Carlo
MD	=	Molecular dynamics
Mequiv	=	Milli equivalent
MSD	=	Mean square displacement ($Å^2$)
N	=	Number of molecule
NVT	=	Carnonical ensemble
ns	=	Nano second (10^{-9} s)
S	=	Semens
T	=	Temperature (K)
V	=	Volume ($Å^3$)
σ	=	Conductivity (S/cm)

MOLECULAR DYNAMICS SIMULATION OF ION CONDUCTION IN CHITOSAN MEMBRANE FOR PEM FUEL CELL

INTRODUCTION

At present, energy consumption continuously increases, but many energy resources have decreased. Many researchers try to find new ways to handle this problem. Fuel cell is one of them because of its advantages such as it is the environmentally friendly electric power sources. Since, it relys on electrochemistry and converted directly to electricity, it is no combustion process and thus no harmful pollutants. Fuel cells work in the same way as conventional battery, but have the major advantage that they do not run down over time and will go on producing electricity as long as this fuel supply does not run out. Using reformer technology, fuel cell can use hydrogen from hydrocarbon fuel, for example natural gas, methanol or even water.

Fuel cells have many types depending on their operations. Proton exchange membrane (PEM) is one of them. PEM fuel cell operates at low temperature, about 70-80 ^{o}C. This can drive them a prime candidate for powering the next generation of electric vehicles, medical devices, and their modular design and the prospects of micro-scaling have gained the attention of cell phone and laptop manufactures. The basic structure and operation principle the PEM fuel cell are illustrated in Figure 1. The PEM fuel cell is constructed by a polymer electrolyte membrane. The membrane and the two electrodes (teflonated porous carbon or cloth with platinum on supported carbon) are assembled into a sandwich structure to form a membrane electrode assembly (MEA). The MEA is placed between two graphite bipolar plates with machined that provide flow channels for disturbing the fuel (hydrogen) and oxidant (oxygen from air). The hydrogen rich fuel is fed to the anode, where the hydrogen diffuses through the porous gas diffusion electrode (GDE). At the catalyst layer, the hydrogen splits into hydrogen proton (H^{+}) and electrons according to:

$$2H_2 \rightarrow 4H^+ + 4e^- \quad (1)$$

driven by an electric field, the H^+ ions migrate through the polymer electrolyte membrane. The oxygen in the cathode gas stream diffuses through the gas diffusion electrode towards the catalyst interface where it combines with the hydrogen protons and the electrons to form water according to:

$$O_2 + 4H^+ + 4e^- \rightarrow 2H_2O \quad (2)$$

The overall reaction is exothermic and can be written as:

$$2H_2 + O_2 \rightarrow 2H_2O + \text{electricity} + \text{heat} \quad (3)$$

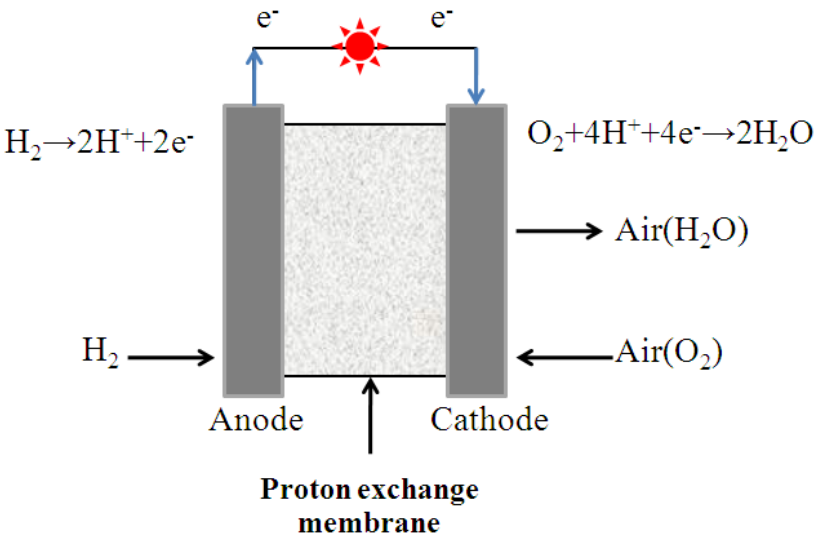

Figure 1 Schematic of PEM Fuel Cell.

The performance of the cell is influenced by many factors. The major performance can be improved by chemical structure of membrane which has directly affected to proton transfer. The polymer membranes, which are commercially available, are based on perfluorinate sulfonic acid polymer such as Nafion. This polymer electrolyte consists of a perfluorinated polymer backbone with sulfonic acid side chains. When fully humidified, this material becomes an excellent protonic conductor. Therefore, there are many researchers have concerned with the polymer

membrane and tried to find the best membrane giving the best performance of the cell.

Many researchers studied the alternative polymers for better conductivity. One substituted for synthetic polymer is natural polymer called chitosan. Chitosan is the derivative of chitin that is a natural polysaccharide that occurs mainly in insects, marine invertebrates, fungi and yeasts. It is also abundant natural polymers next to cellulose. When the N-deacetylation was occurred, chitin was converted to citosan as shown in Figures 2 and 3. However, the N-deacetylation processing is almost never completed. In addition, the degree of deacetylation (DDA), which determines the content of free amino groups in the polysaccharides, can be employed to differentiate between chitin and chitosan. Thus, properties of chitosan rely on the amino group and hydroxyl group in their structure. Chitosan can be characterized in terms of its quality, intrinsic properties (purity, molecular weight, viscosity, and degree of deacetylation) and physical forms. There are some researches studying the possibility of using chitosan as the membrane for PEM fuel cell (Mukoma *et al*., 2004 and Wan *et al*., 2003). Ennari *et al*. (2001) studied the mechanism of the ionic conductivity of poly (ethylene oxide) sulfonic acid anion by using the atomistic molecular modeling technique.

The widespread availability and use of preference computer has resulted in molecular modeling and simulation techniques becoming a common research tool. Computational techniques are being used to study the science behind fuel cells, helping researchers get better understanding processes and experiment with the new approaches. Molecular modeling and simulation has been used to study new electrolyte material and surface catalysis for fuel cells.

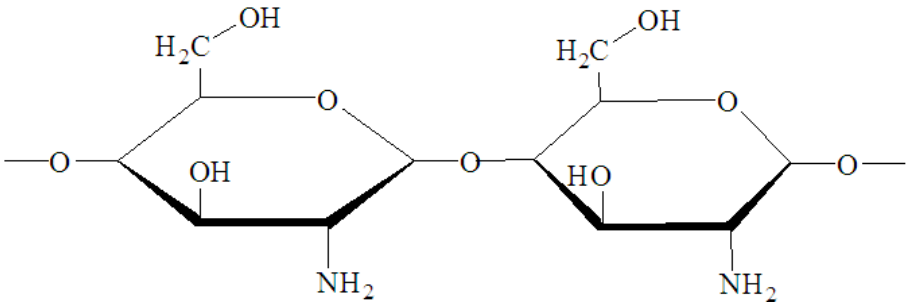

Figure 2 Molecular structure of chitosan.

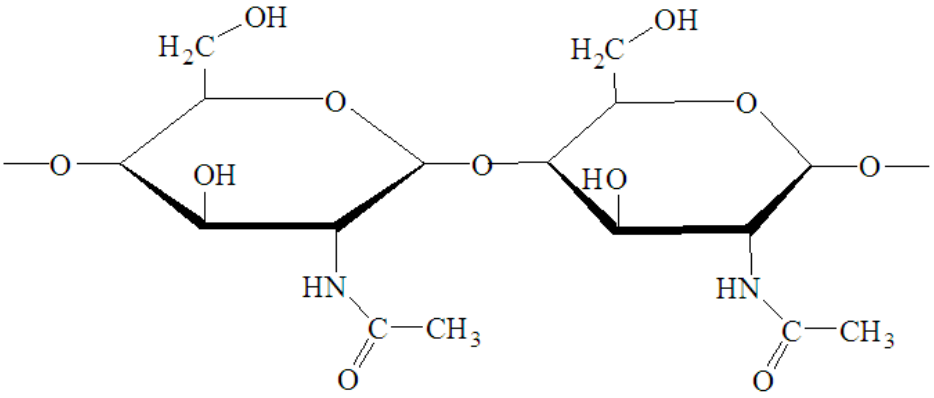

Figure 3 Molecular structure of chitin.

The goal of this work is to calculate the ion conductivity of chitosan as the membrane of PEM fuel cell with different amount of water in molecular level and various DDA. Molecular Modeling technique can create the amorphous system which composes of chitosan molecule, hydronium ion (refer to hydrated proton) and water molecule. Molecular dynamic results present the dynamical data to calculate the ion conductivity and the coordination data to study the transport mechanism of the ion.

OBJECTIVE

1. To study and simulate the diffusivity and ion conductivity of chitosan membrane system for PEM fuel cell by molecular modeling technique.

2. To study the transport mechanism of the ion through chitosan membrane by coordination data.

3. To compare the conductivity from simulation with reference reported experimental data.

Scope of work

1. The simulator named Material Studio 4.3 software will be the main tool for modeling, simulation and implementation.

2. The transfer ion, hydronium ion was used in place of hydrated proton in this study.

3. The system of chitosan membrane is studied in the range of 10-40 wt% of water and 298-360 K. Chitin presented in chitosan with various degree of deacetylation (DDA), 70 – 90 DDA, were studied.

4. Molecular modeling is also concerned with more ideal models, some of which have distinguished properties and differentiate from a real system.

Thesis Contributions

1. The molecular modeling and simulation can determine the mechanism and transport phenomena in PEM fuel cell for improvement of the cell.

2. This method is a basic for design and production of PEM fuel cell manufactures.

3. The molecular modeling technique is able to find the new materials for polyelectrolyte membrane.

LITERATURE REVIEW

1. Proton exchange membrane (PEM)

Proton exchange membrane, polymer exchanged membrane, conducting polymer and polyelectrolyte, these words are the same synonyms. There are many researcher devote for improving PEMs. PEM fuel cells are being developed for three main applications: automotive, stationary, and portable power. Each of these applications has its unique operating conditions and materials requirements. PEM fuel cells rely on absorbed water and its interaction with acid groups to produce protonic conductivity. The material used historically and most frequently in PEM fuel systems is Nafion, a perfluorocarbon-based polymer carrying sulfonic acid residues. Nafion is a commercial material and has received the most extensive study of any PEM fuel cell membranes. Other polymer systems that would have even better performance than Nafion and/or have lower costs are being sought by researchers around the world. Hickner *et al*. (2004) proposed the alternative polymer systems for proton exchange membranes. The Nafion and other poly(perfluorosulfonic acid) membranes, PEMs containing Styrene and its derivatives, poly(arylene ether)s, PEMs Based on Poly(imide)s and Polyphosphazene PEMs were studied, and also the suggestion considerations in design new PEMs. Many families of polymers with differing chemical structures and various strategies for incorporation of sulfonic acid groups have been explored as proton exchange membrane materials. Most reports of new materials have included information on ion content, protonic conductivity, and water uptake. Despite the large body of research on this topic, there are a few basic polymer properties that are still not well-known for common systems or not measured in most reports. Perhaps the most glaring omission in new ion conducting polymer research is the characterization of molecular weight. Molecular weight is one of the most basic properties of polymeric materials. The ion effect on chain size is often termed as the polyelectrolyte effect. These types of materials have complex transport properties that involve not just proton movement, but also the movement of water. Theoretical treatments of the transport mechanisms and processes in these proton conductors are given by Kreuer *et al*. (2004)

2. Chitosan with PEM

Chitosan is the biopolymer more functional in wide application, such as medication, agriculture, nutrition, cosmetic, textile, pulp and paper, coating material and conducting polymer. Kumar (2000) took a closer look at chitin and chitosan applications in a review. He purposed the processing of chitin and chitosan, the alkali removes the protein and deacetylates chitin simultaneously. The processing of crustacean shells mainly involves the removal of proteins and the dissolution of calcium carbonate which is present in crab shells in high concentration. The resulting chitin was deacetylated in 40 % sodium hydroxide at 120 ^{o}C for 1- 3 hour. This treatment produced 70 % deacetylated chitosan. However, the deacetylation processing is never completed.

This research focused in conducting polymer especially ion transfers through the chitosan membrane. There are many researcher worked intensively to improve the new polyelectrolyte membrane. Wan *et al*. (2003) had investigated the ion conductivity of chitosan membrane. The chitosan membranes with the various degrees of deacetylation and deifferent molecular weights (MW) were prepared by film casting with the aqueous solutions of chitosan and acetic acid. Ultraviolet (UV) spectrometry and infrared (IR) spectrometry were used to determine the degree of deacetylation (DDA) of chitosan. The viscosity-average MW of chitosan was measured in an aqueous solvent system of 0.25 M CH_3COOH/0.25 M CH_3COONa. The intrinsic ionic conductivities of the hydrated chitosan membranes were investigated using impedance spectroscopy. It was found that the intrinsic ionic conductivity was as high as 10^{-4} S/cm after hydration for 1 h. The tensile strength and breaking elongation of the membranes were evaluated according to standard ASTM methods. The crystallinity and swelling ratio of the membranes were examined. A tentative mechanism for the ionic conductivity of chitosan membranes was also suggested.

Ramirez *et al*. (1997) had built the model of membrane for determining membrane potential and ionic flux in weak amphoteric polymer membranes. They presented model calculations concerning the membrane potential and ionic fluxes in

weak amphoteric polymer membranes. They mentioned that the results were compared with experimental data obtained with a membrane which contained succinyl-chitosan as ampholyte and poly (vinyl alcohol) as supporting matrix. The ion transport through the membrane had been described with the aid of the Nernst-Planck equations, and the result obtained explained satisfactorily the observed experimental trends in broad ranges of pH and electrolyte concentration. Also, the model predictions concerning the membrane isoelectric point might be useful for the analysis of future experiments.

Chitosan membrane has been compared with the Nafion. Mukoma *et al*. (2004) investigated the proton conductivity of chitosan membrane used for the membrane of Proton Exchange Membrane fuel cell (PEMFC). Chitosan membranes cross-linked in sulfuric acid were evaluated for their thermal stability, water absorption. They mentioned that Chitosan membranes were found to be more hydrophilic than Nafion 117 in water uptake experiments. Chitosan membranes absorbed about 60% water on average compared with the 30% for Nafion 117. Preliminary TGA/DSC thermal stability studies showed that after the initial weight loss due to water, chitosan membranes decomposed in three stages with the final stage beginning at about 300 ^{o}C. Chitosan membranes proton conductivities under various temperature and humidity conditions were reported and compared with that for the commercial membrane Nafion 117. Partially-hydrated chitosan membranes at ambient temperature displayed a proton conductivity of about 0.005 S/cm as oppose to 0.08 S/cm for Nafion 117 under the same conditions. At 60 ^{o}C (full hydration) Nafion 117 membranes had a conductivity of about 0.12 S cm^{-1} and chitosan membranes have 0.02 S cm^{-1}.

Moreover, application of chitosan with other materials was studied by Yamada and Honma (2005) and Ramírez-Salgado (2006). They worked to improve the electrical and mechanical properties of membranes with a low cost of production. The biopolymer could be an answer to produce proton membranes at low cost.

Yamada and Honma (2005) investigated a low production cost anhydrous proton conductor consisting of chitosan and methanediphosphonic acid (MP). This

chitosan-200 wt% MP composite material showed the high proton conductivity of 5×10^{-3} S/cm at 150 ^{o}C under anhydrous conditions. Ramírez-Salgado (2007) demonstrates that the intrinsic membrane polymer and clays properties could help to develop a novel proton exchange membranes. Biopolymer composites (chitosan-oxide compounds) present conductivity between 10^{-3} and 10^{-2} S cm^{-1}. The measurements were calculated by EIS (1MHz-0.05 Hz) using the two electrode configuration. Different oxides were used: MgO, CaO, SiO_2, Al_2O_3. The ionic conductivities were compare with Nafion‘s in the same condition of P and T. The catalyst layer/membrane ensemble was made during the design with the subsequent demonstration as membrane electrode essemblies and finally the fuel cell was built. Their focus was to increase the compatibility between the proton basic polymer exchange membrane and basic clays as CaO and test a new kind of fuel cell.

3. Molecular modeling with PEM

Today, molecular modeling is invariably associated with the computer modeling, but it is quite feasible to perform some simple molecular modeling studies using mechanical models or a pencil, paper and hand calculator. Nevertheless, computational techniques have revolutionized molecular modeling to the extent that most calculations could not be performed without the use of a computer. This is not to imply that a more sophisticated model is necessarily any better than a simple one, but computers have certainly extended the range of models that can be considered and the systems to which they can be applied. The model that most chemists first encounter is molecular models. These models enable three-dimensional representations of the structures of molecules to be constructed. These structural models continue to play an important role both in teaching and in research, but molecular modeling is also concerned with more abstract models. An obvious example is quantum mechanics, the foundations of which lay many years before the first computers were constructed.

Conductivity of chitosan membrane has been studied by molecular modeling dividing into two branches. First, molecular modeling was used to study transfer mechanism through hydrogen bond or Grotthus mechanism. Second, molecular dynamics was used to study transport properties of the particles through the membrane without creating and breaking bond.

This section will concern about Grotthuss mechanism or interaction between water, hydronium ion or any particles and fixed group of membranes. Paddison and Elliott (2007) evaluated the hydration of the short-side-chain perfluorosulfonic acid membrane through a comparative study of the energetic of an oligomeric fragment of the polymer using ONIOMDFT/HF molecular orbital calculations. Extensive searches for minimum energy conformations of the three pendant side chain oligomeric fragment of the polymer, $CF_3(CF(-O(CF_2)_2 SO_3 H)(CF_2)_7)_2 CF(-O(CF_2)_2 SO_3 H)CF$, at the B3LYP/6-31G** :HF/3-21G** level with from 6 to 9 explicit water molecules revealed that at the lower range of the examined hydration (i.e. $2H_2O/SO_3 H$) the uniform hydration of the sulfonic acid groups results in the lowest energy and therefore most favorable state of the system. Their calculations showed, however, that as the degree of hydration is increased the energetic preference for uniform hydration decreases, disappearing altogether at 3 H_2O/SO_3H. Furthermore, they found that water distributions that facilitate a higher degree of dissociation and separation of the protons are important factors instabilizing the fragments. These calculations provide a base line set of results for which the effects of distinct backbone and side chain chemistry may be explored on hydration in minimally hydrated candidate polymer electrolyte membranes.

Kim *et al*. (2008) proposed a new type of sulfonated aromatic polyarylenes as candidate building blocks for proton exchange membranes. Density functional theory (DFT) calculations and *ab initio* molecular simulations (BLYP/6-31G**) suggest that desulfonation is limited at high temperatures, owning to the strong aryl-SO_3H bond induced by the electron deficient aromatic ring, and that proposed polymers exhibit good thermodynamical stability due to the robust aromatic main-chain repeating unit. Simulations also emphasize the importance Grotthus-type mechanism, with interconversion between Eigen ($H_9O_3^+$) and Zundel cations ($H_5O_2^+$) as limiting structures, for the hydrated proton transport in the vicinity of the sulfonic acid groups.

The above examples used the molecular orbital calculation which search for minimum energy conformations and predicted. This method deals with the electrons in system, so that even if some of the electrons are ignored a large number of particles must still be considered, and the calculations are time-consuming. Force field

methods (also known as molecular mechanics) ignore the electronic motions and calculate the energy of a system as a function of the nuclei positions only. The total potential energy consists of stretching of bond, bending of angle, torsion and non-bond interaction terms written as (Venkatnathan *et al*., 2007)

$$E_{total} = E_{bond} + E_{angle} + E_{torsion} + E_{nonbond}$$

In principle, the above equation could be solved for the potential energy *E* an empirical fit to the potential energy surface, commonly called a forcefield is used. Since the nuclei are relatively heavy objects, quantum mechanical effects are often insignificant, in which case molecular dynamics can be used.

There are many researchers who developed theoretical and methodology to predict the ion conductivity of PEM. López-Chávez *et al*. (2005) developed a theoretical methodology to describe the ion conductivity mechanism of chitosan membrane and to obtain its magnitude. Atomistic molecular modeling has been utilized to construct an ionic conducting polymer-electrolyte system consisting of chitoan, H_2O molecules and H_3O^+, OH^-, SO_4^{2-} ions, inside of simulation cell. The COMPASS force field was used. The simulation allows describing the ionic conductivity mechanism along the polymer matrix. The theoretical results obtained are compared with previously reported experimental data for chitosan membranes. They suggest that the percent of water and sulfates might improve the ionic conductivity in chitosan membranes until a value 2×10^{-2} S/cm. The present methodology can be considered as a first step towards understanding these complex problems of technological interest.

On the other hand, many types of PEM have been studied in molecular method. Pozuelo *et al*. (2006) used the molecular dynamics to simulate separately the diffusion of nacked protons and hydronium ions across the sulfonated poly(phenyl sulfone)s using PCFF force field. Simulations were carried out for wet membranes with the following characteristics: ion-exchange capacity, 1.8 mequiv/g of dry membrane; water uptake, 10-30%; temperature range, 300-360 K. The diffusion coefficient of nacked protons is nearly 1 order of magnitude higher than that of the

hydrate protons for the membranes with the lower water uptake (10%). For the membrane with higher water uptake the ratio between the diffusion coefficients of the two particles reduce to about half an order of magnitude. The conductivity of the naked protons increased from 21.4×10^{-3} to 52.5×10^{-3} S/cm when the water uptake increases from 10% to 30%. For hydrated protons the conductivity increases from 1.54×10^{-3} to 7.57×10^{-3} S/cm. The conductivities obtained through simulations carried out at 300 K for the hydrate proton across membranes with water uptake 18% and 30% are roughly similar to those experimentally measured for a membrane with ion exchange capacity 18 mequiv/g and water uptake equal to 24.3%. Simulation conductivities of both naked protons and hydrate protons follow Arrhenius behavior.

There is one example for long research and developing methodology to study polyelectrolyte materials. Ennari *et al*. (1999) had used the atomistic molecular modeling to construct a proton-conducting polymer electrolyte system consisting of poly(ethylene oxide) sulfonic acid anion (PEO sulfonic acid anion), water, hydronium ion and proton in an amorphous cell. The forcefield was parameterized to simulate proton transport as accurately as possible in an atomistic model. The coordinate study was made and found to be mainly in accordance with experimental data. The diffusion coefficients for the PEO sulfonic acid anion, water, the proton and for hydronium ion were determined. The ion conductivities of the whole system and of the ions were estimated and found to be in accordance with experimental values. The good correlation between the experimental and simulated results shows that the used model may provide guidance for evaluating new materials by experimentalists. Two year later Ennari *et al*. (2001) had used the molecular modeling to construct amorphous 35.0 wt% water-containing polymer electrolyte materials consisting of two polymers: poly(ethylene oxide) (PEO) and poly(ethylene oxide) with sulfonic acid anion end groups (PEO sulfonic acid anion). The cations in the system were the hydronium ion, which simulates the classical diffusion of the hydronium ion and proton, which simulates the proton hopping mechanism. The possible of the ions to move together with the polymer the polymers in the matrix was also discussed. The coordination between the ions were calculated and compared with the results for similar systems having different amounts of water. The diffusion coefficients for the ion and the

conductivity of the system were calculated. The system was found to be conducting, which agrees with the experimental work. In the simulation, both the hopping and the diffusion mechanism were important in the studied system, while in the simulated system, which contains only one PEO sulfonic acid anion in water, the hopping mechanism dominated. The good correlation between the experimental and simulated results shows that the used model is able to estimate whether the material is conducting or non-conducting. The model can also offer interesting information concerning the possible mechanisms of proton conductivity in polymer electrolyte materials. In 2008, Ennari had used atomistic molecular modeling to constructed PVF-based polyelectrolyte materials containing 0, 10 or 40 wt% of water. The system contained hydronium ions, with which classical diffusion of hydronium ions could be simulated, and particles called protons, with which the proton hopping mechanism could be simulated. System containing 40 wt% of water was conducting. Both the proton hopping and classical diffusion mechanism occurred in the system and neither of them was dominating. The interactions between ions were calculated and they were found to be relative small. Diffusion coefficients of the protons, hydronium ions and water molecules were reported and the movement of the ions is studied. The location of the protons, the hydronium ions and water molecules was studied at the atomistic level. In system containing 40 wt% of water, water clusters are seen. There were no remarkable differences between the results that were measured for similar materials or calculated in their study.

Devanathan *et al*. (2007b) have performed a detailed and comprehensive analysis of the dynamics of water molecules and hydronium ions in hydrated Nafion using classical molecular dynamics simulations with the DREIDING force field. In addition to calculating diffusion coefficients as a function of hydration level, they have also determined mean residence time of H_2O molecules and H_3O^+ ions in the first solvation shell of SO_3^- groups. The diffusion coefficient of H_2O molecules increased with increasing hydration level and was in good agreement with experiment. The mean residence time of H_2O molecules decreases with increasing membrane hydration from 1 ns at a low hydration level to 75 ps at the highest hydration level studied. These dynamical changes are related to the changes in

membrane nanostructure reported in the first part of the work. Their results provide insights into slow proton dynamics observed in neutron scattering experiments and are consistent with the Gebel model of Nafion structure.

Selvan *et al*. (2008) used the molecular dynamic simulation examine the structural and transport properties of water and hydronium ions at the interface of Nafion polymer electrolyte membrane and vapor phase. The effect of humidity was studied by examining water contents of 5, 10, 15 and 20 % by weight. They observed a region of water depletion in the membrane near the vapor interface. The vehicular diffusion of hydronium ions and water as components parallel and perpendicular to the interface were reported. In the interfacial region, for hydronium ions, they find that the component of the vehicular diffusivity parallel to the interface was largely unchanged from that in the bulk hydrated membrane, but the component perpendicular to the interface has increased, due to local decrease in density. The similar behavior with water in the interfacial region was found. On the basis of these diffusivities, they concluded that there is no observable additional resistance to mass transport of the vehicular component of water and hydronium ions due to the interface. In terms of structure at the interface, they found that there is a decrease in the fraction of fully hydrated hydronium ions. This translates into a lower probability of forming Eigen ions, which are necessary for structural diffusion. Finally, they observe that the hydronium ions display a preferential orientation at the interface with their oxygen atoms exposed to the vapor phase.

MATERIALS AND METHODS

1. Construct the system various amount of water and temperature.

The materials of conducting polymer were constructed and simulated by means of the Accelrys commercial software (Materials Studio 4.3 licensed from NANOTECH Thailand) using the COMPASS force field. The amorphous builder module was used to construct the system and then the minimization, molecular dynamic were analyzed by discover module. First, water molecule and hydronium ion were constructed and minimized by steepest-descent method as shown in Figure 4. Chitosan monomer was constructed and the polymer builder module was used to construct chitosan chain by 10 repeating unit and minimized by steepest-descent method as shown in Figure 5. Then, the 3D amorphous systems with periodic boundary conditions and containing chitosan polymer chain with 10 repeating unit, hydronium ion and various amounts of water were built using the Amorphous cell module as shown in Figure 6. The composition of each cell is summarized in Table 1. All the system contained two chains of polymeric chitosan each one with 10 amino groups. All the system contained also twenty hydronium ions and 10, 20, 30 and 40 wt% of water.

Table 1 Description of the different simulated cell.

Cell	Number of particle			wt% of water	Volume of cell ($Å^3$)
	Chitosan(10)	H_2O	H_3O^+		
Cell 1	2	23	20	10	5176.64
Cell 2	2	52	20	20	5843.672
Cell 3	2	90	20	30	6717.889
Cell 4	2	135	20	40	7752.987

In the minimization and optimization of the geometries and finally of the structure an equation describing the energy of the system as a function of the coordinates of the system, (a potential energy function), is first defined. In this study the COMPASS forcefield defines this function and the parameters needed to calculate the potential energy surface for the system (Sun, 1998, Bunte and Sun, 2000). Next a minimization algorithm is chosen to find the potential energy minimum of the potential energy surface corresponding to the lower energy structure. Usually after many iterations this lead to the optimized structure and, thus, to find the optimal structure the coordinates of the initial structure are changed several times.

2. Minimization and molecular dynamics

All the systems were minimized by using the steepest-descent method until the maximum derivative 0.1 kcal/mol was reached. After minimization, a molecular dynamics run was made using the NVT ensemble and Andersen for temperature control. The temperature used in the dynamics was 298, 320, 340 and 360 K. The time step was 1.0 fs and 200 ps long dynamics runs to study the dynamical properties of these cells. The van der Waals and coulombic nonbonding interactions were calculated by the Ewald summation method.

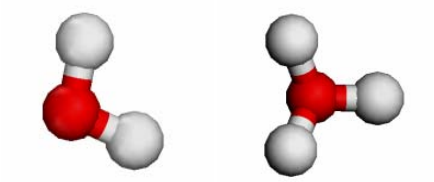

(a) (b)

Figure 4 Water molecule (a) and hydronium ion (b).

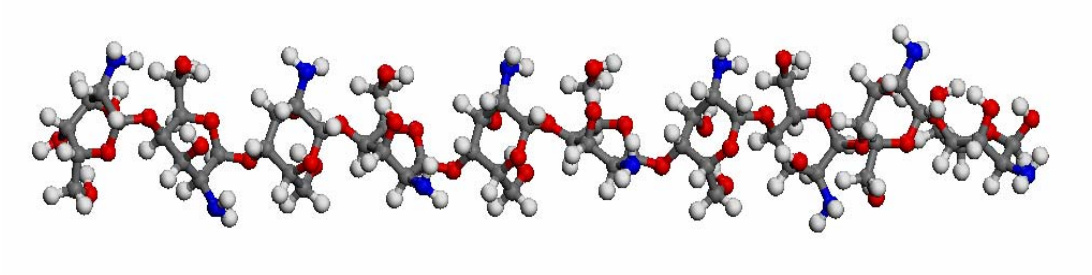

Figure 5 Chitosan chain with 10 repeating units.

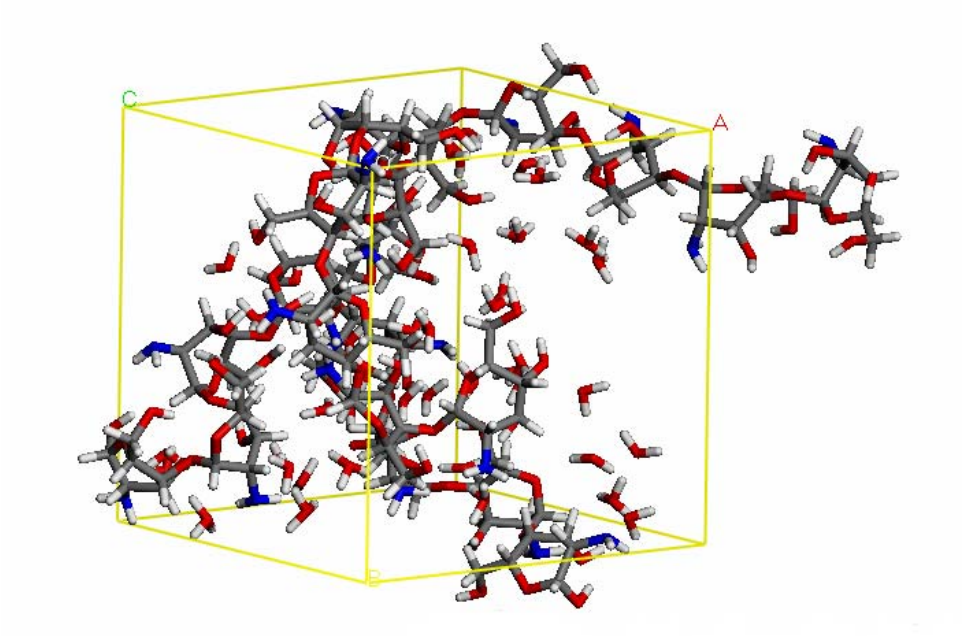

Figure 6 An amorphous system with 10 wt% of water.

The dynamic of particles may be investigated through the continuous solution of Newton's equation (classical molecular dynamics) or with stochastic methods including Monte Carlo (MC) theory (Leach, 1996). Classical MD simulations with empirical potentials can handle systems consisting of thousands of particles over time periods of nanoseconds and have been used to study proton transport in materials as a function of parameters such as temperature, water content, and, in polymers equivalent weight and chemical and physical characteristics of main and side chains. The molecular dynamics simulation step can be divided into four stages. In the initialization stage the Cartesian coordinates are set. In the heating stage the kinetic energy is slowly added to the system by calculating the distribution of the atomic

velocities using the Maxwell-Boltzmann equation. In the equilibration stage the velocities are scaled by the Andersen method to maintain the desired temperature. In the production stage the observable values are calculated and saved.

The MD was realized by using COMPASS forcefield, which is the first *ab initio* forcefield that has been parameterized and validated using condensed-phase properties, in addition to various *ab initio* and empirical data for isolated molecules (Sun, 1998). Consequently, this forcefield enables accurate prediction of structural, conformational, vibrational, ionic conductivity and thermo physical properties for a broad range of molecules in isolation and in condensed phases.

3. The Diffusion coefficient and ion-conductivity.

After molecular dynamics runs, the mean-square displacement or MSD were calculated that obtain the diffusion coefficient and ion conductivity respectively.

The diffusivity is given by

$$D_\alpha = \frac{1}{6N_\alpha} \lim_{t\to\infty} \frac{d}{dt} \sum_{i=1}^{N_\alpha} \langle [R_i(t) - R_i(0)]^2 \rangle \tag{4}$$

The sum term of the right hand side divided by N_α is the mean square displacement (MSD). N_α is the number of diffusing particles α, t is time and $R_i(t)$ is the position vector of particle α at time event t. Equation (4) is valid only when the Einstein diffusion is reached. This means that the motion of diffusing particle follow a random walk, e.g. the motion of particle is not correlated with its motion at any previous time. To test the equation (3) is valid, log MSD against log time was plotted in each case. The slope of curve is 1.0±0.03, when the Einstein diffusion is reached.

The ion conductivity, σ, has been evaluated by using the Einstein equation

$$\sigma = \frac{Nz^2e^2D}{VkT} \tag{5}$$

where σ is the ion conductivity, N is the number of counterion in the simulation cell, V is the simulation cell volume, k is Boltzmann's constant, z is the total charge in unit of e, e is the elemental charge. (Pozuelo *et al*., 2006)

4. Conductivity of chitosan with various degrees of deacetylation

Chitosan is derived from chitin, in natural chitosan never pure completely. Thus, the conductivities of chitosan various degrees of DDA were calculated. First, the 3D amorphous systems with periodic boundary conditions and containing chitosan polymer chain with 9 repeating unit and one chitin unit (90%DDA), hydronium ion and water molecule were built using the Amorphous cell module. The 3D amorphous system of chitosan polymer chain with 8 repeating unit and two chitin unit (80%DDA) and chitosan polymer chain with 7 repeating unit and three chitin unit (70%DDA) were constructed respectively. The composition of each cell is summarized in Table 2. All the systems were minimized and molecular dynamics run like as step 2. The Diffusion coefficient and ion-conductivity were calculated like as step 3.

Table 2 Descriptions of the different simulation cell with various degree of deacetylation.

System	Number of particle			Wt% of water	Volume of cell (Å^3)
	H_3O^+	H_2O	Chitosan		
DDA90	20	138	2	40	7929.409
DDA80	20	141	2	40	8105.823
DDA70	20	144	2	40	8282.113

5. The pair correlation study

After the molecular dynamic was run, the pair correlation function was analyzed to study the location of the particles in the system. Radial distribution functions or pair correlation functions are a useful way to describe the structure of a

system, particularly of liquids. Consider a spherical shell of thickness *dr* at a distance *r* from a chosen atom. The volume of the shell is given by:

$$V=\frac{4}{3}\pi(r+dr)^3-\frac{4}{3}\pi r^3$$

$$V=4\pi r^2 dr+4\pi r dr^2+\frac{4}{3}\pi dr^3\approx 4\pi r^2 dr$$

If the number of particle per unit volume is ρ, then the total number in the shell is $4\pi\rho r^2 dr$ and so the number of atoms in the volume element varies as r^2.

The pair distribution function, *g(r)*, gives the probability of finding an atom or molecule a distance *r* from another atom or molecule compared to the ideal gas distribution, *g(r)*, is dimensionless. The radial distribution function calculated from a molecular dynamics simulation. Then, the coordination number was calculated as follows;

$$n_{AB}=\int_0^r 4\pi\rho r^2 g_{AB}(r)dr \qquad (6)$$

where n_{AB} is the number of *A* particles coordinated to particles *B* within a radius *r*. The coordination number is the area under the curve between the pair correlation function, *g(r)* against distance, *r* (Leach, 1996).

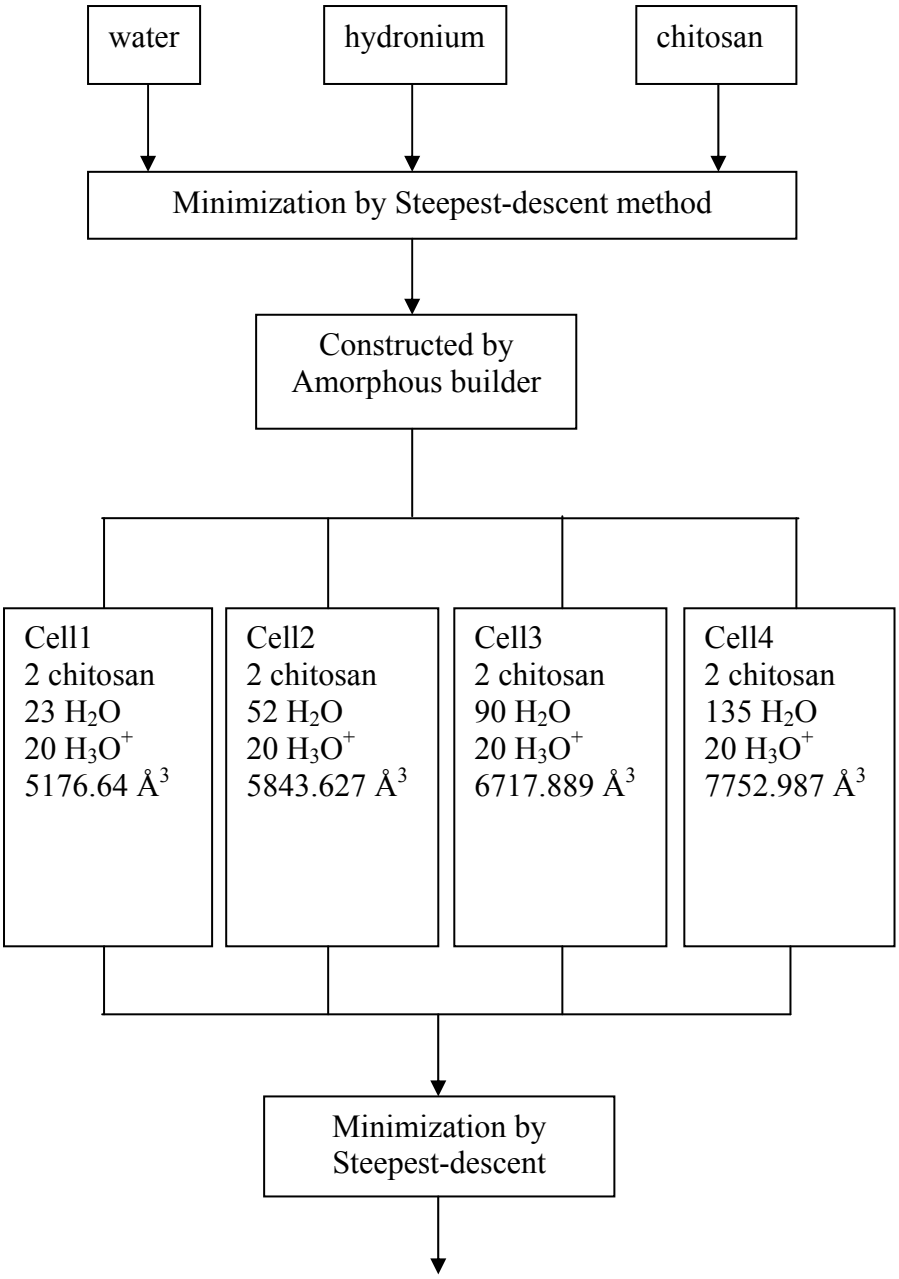

Figure 7 Scheme of the working step for this research

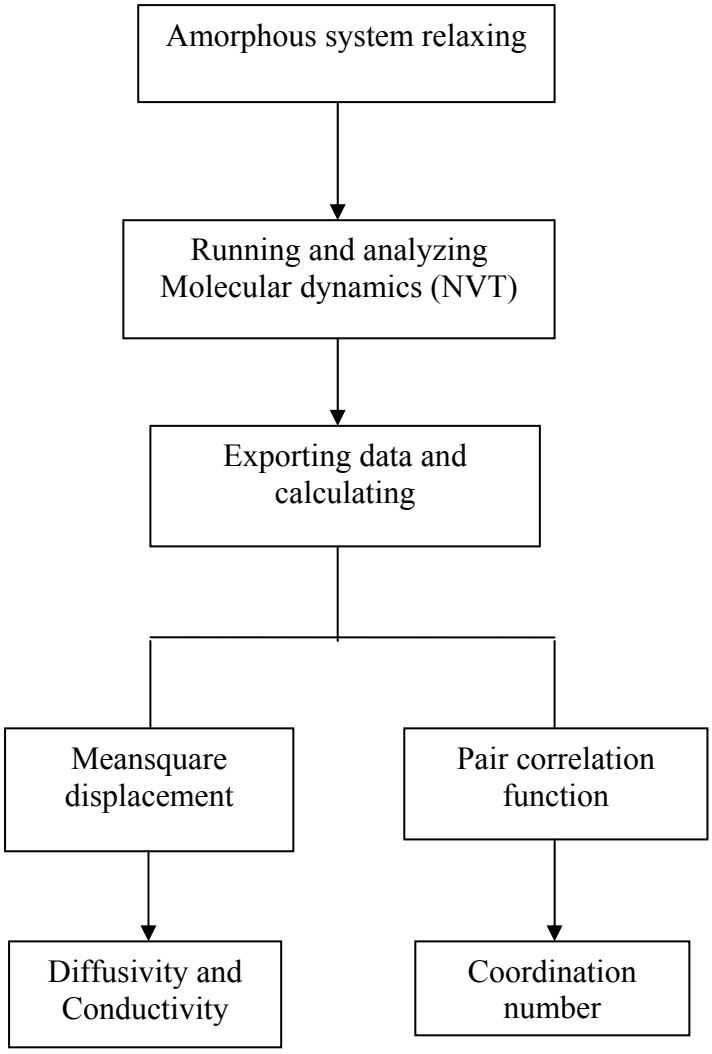

Figure 7 (Continued)

RESULTS AND DISCUSSION

In this section, the computational results will be discussed, includes the minimization energy of all structure and systems, the ion conductivity and transport mechanism. The ion conductivity was calculated by the dynamical information. The transport mechanism of the ion was considered by the coordination data.

1. Energy Minimization

In molecular modeling we are especially interested in minimum points on the energy surface. Minimum energy arrangement of the atoms corresponds to stable states of the system. Energy minimization section divided in two parts, minimum structures and minimum systems. Firstly, chitosan conformation was constructed by polymer builder module with 10 repeating unit, head to tail and isotactic structure. Moreover the minimization energy was calculated by steepest-descent method as shown in Figure 8. The potential energy will decrease until optimum structure can be obtained with the lowest molecular energy. The step minimization of chitosan structure is 5,000 steps which begin stable at 1,000th step with total energy of 420 kcal/mol. When the molecular energy is low enough, the structure is relaxed and stable. The optimum structure of chitosan was shown in Appendix A.

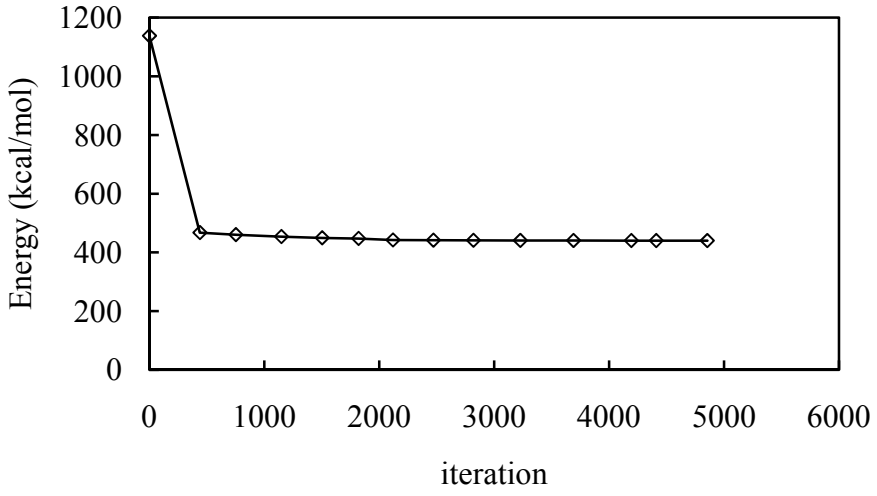

Figure 8 Minimization energy of pure chitosan structure.

Chitosan is N-deacetylated derivative of chitin. In this study, many chitosan membranes with various degree of deacetylation (DDA) were constructed by substituting one H of amino ($-NH_2$) group with acetyl ($-COCH_3$) group. Minimization energy of 90% DDA, 80% DDA and 70% DDA are shown in Figure 9. Their optimum structures illustrated in Appendix A. The potential energy decreases during molecular minimization. The molecular energy of 90% DDA structure is 400 kcal/ mol. The molecular energy of 80% DDA and 70% DDA structures are 350 kcal/ mol and 300 kcal/mol respectively. Figures 8 and 9 indicate that minimization energy increase when DDA increases or acetyl group decreases. This is due to the energy of N-substituted group is less than the amino group. The acetyl group ($-COCH_3$) facilitates withdrawn electron density from N atom.

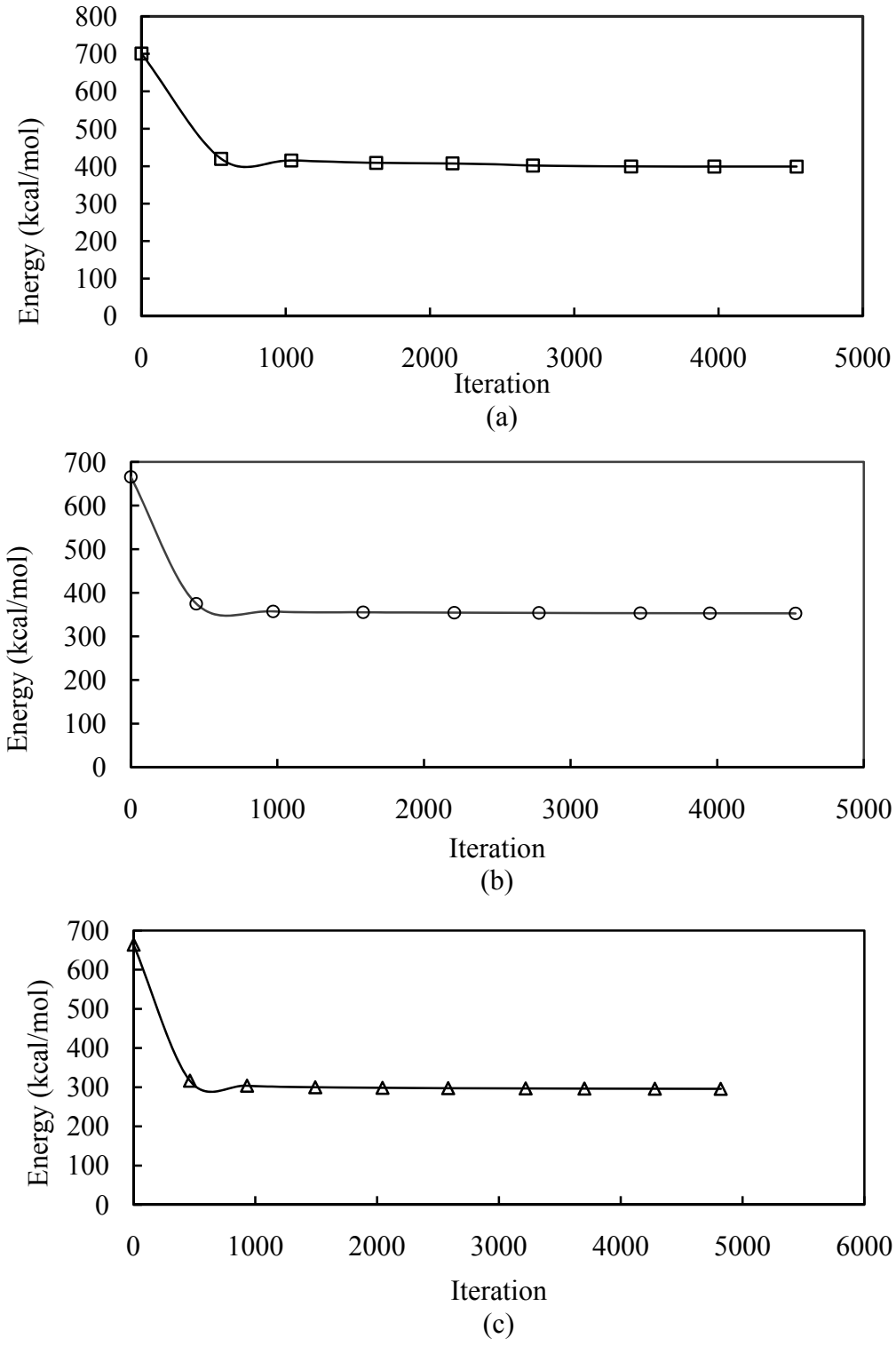

Figure 9 Minimization energy of 90% DDA (a), 80% DDA (b) and 70% DDA (c).

After minimization of each molecule, the amorphous systems were constructed with periodic boundary condition and density 1.3004 g/cm^3. The minimization energy of each system was shown in this part. For Cell1 (10 wt% of water), the potential energy of the amorphous system is -1,400 kcal/mol. The step of minimization is 10,000 steps of which at the 8,000th step it starts to stay as shown in Figure 10. For Cell2 (20 wt% of water), the potential of the amorphous system is -1,800 kcal/mol. The minimization step is 5,000 steps and it begins to stable at the 3,000th step. In Cell3 (30 wt% of water), the potential energy of the amorphous system is -2,200 kcal/mol. The minimization step is 5,000 steps and it starts to constant value at 2,000th step. When the amount of water in the system increased to 40 wt% of water, the potential energy of the amorphous system decreased as shown in Figure10. For Cell4, the minimization energy is -2,700 kcal/mol. The minimization step is 5,000 steps and it begins to stable at the 3,000th step. These information indicate that the number of water molecule cause to declining of total energy of the system.

Figure 11 illustrates the minimization energy in the DDA systems containing 40 % of water. In DDA90 system, the potential energy of the amorphous system is -2,900 kcal/mol. The minimization step is 5,000 steps and reaches to constant value at 2,000th step. In DDA80 system, the potential energy of the amorphous system is -3,000 kcal/mol. The minimization step is 5,000 steps and reaches to stable at the 3,000th step. In DDA70 system, the potential energy of the amorphous system is -3,200 kcal/mol. The minimization step is 5,000 steps and declines to constant value at 2,000th step. The potential energy of the cell decreases when the number of water in the system increases. This is due to the hydrogen bond in the system reduces the potential energy. Such the amorphous cells demonstrated in appendix A.

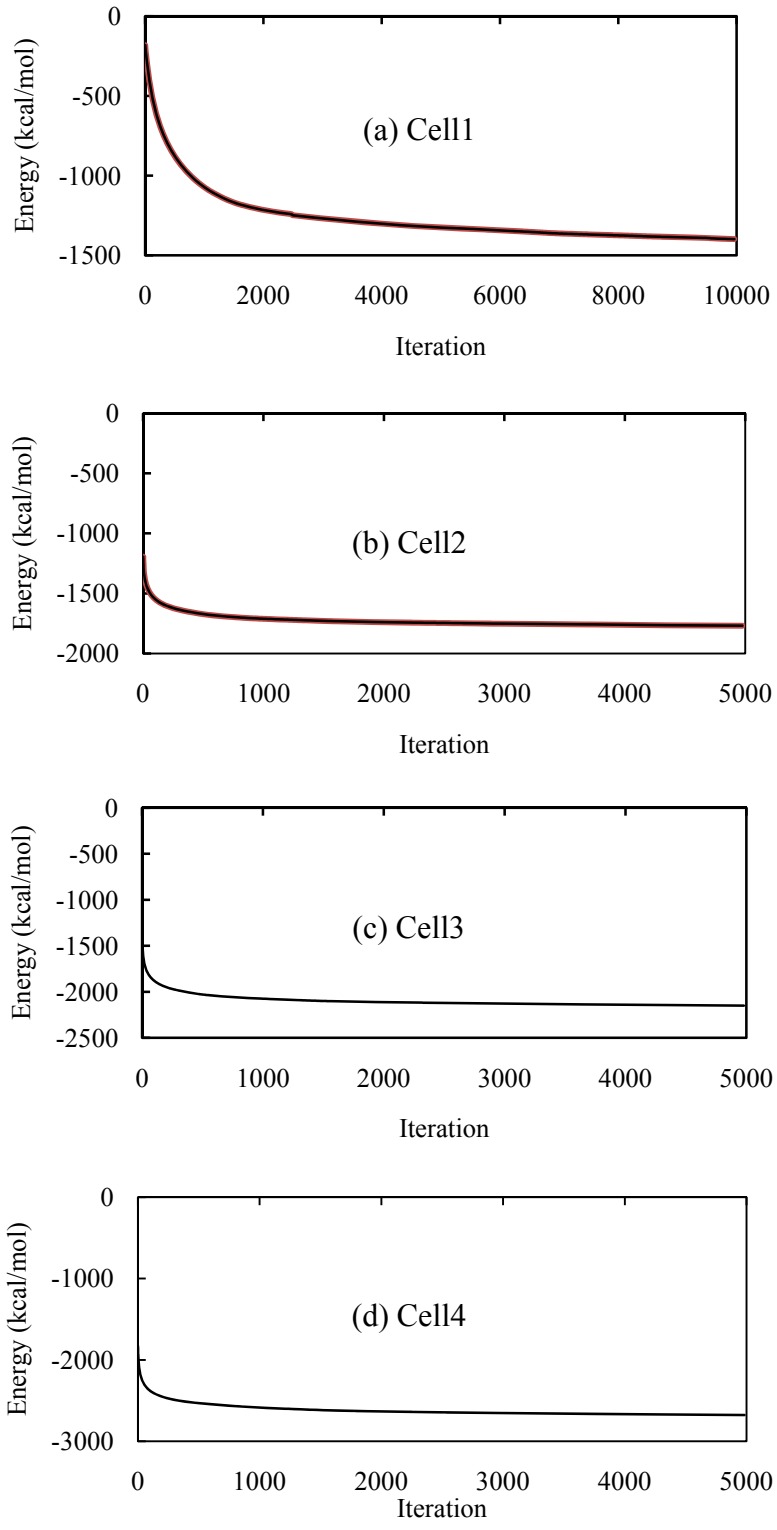

Figure 10 Minimization energy of amorphous system for Cell1 (10 % water) (a), Cell2 (20 % water) (b), and Cell3 (30% water) (c) and Cell4 (40 % water) (d).

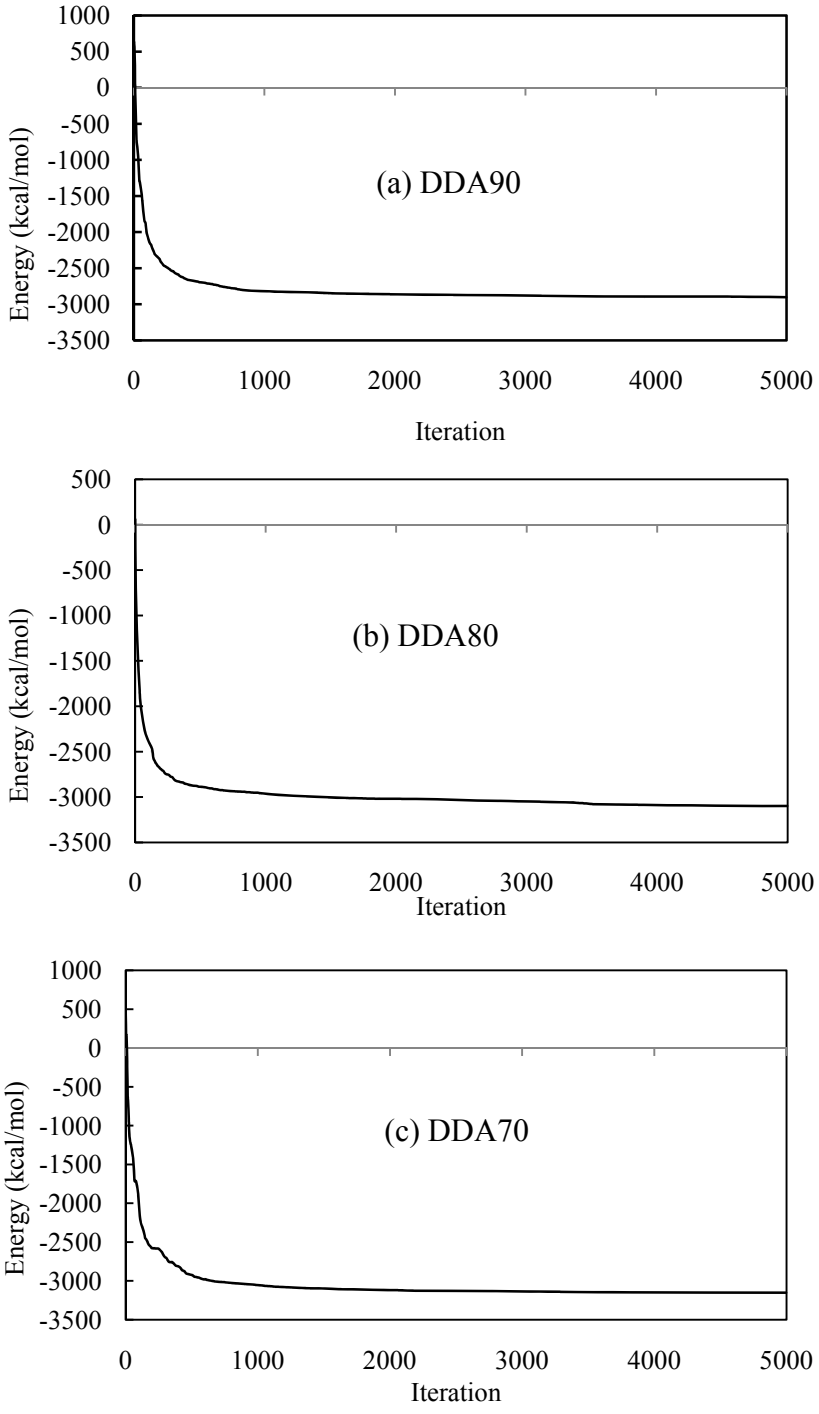

Figure 11 Minimization energy of amorphous system for DDA90 (a), DDA80 (b) and DDA70 system (c).

2. Dynamic properties for Chitosan system

The dynamical study was made to investigate the diffusion of hydronium ion in different systems. The molecular dynamics simulation is used for this study, because it is the most versatile simulation method to study the diffusion in the polymer-based system. However, it has some limitation, e.g. simulations are made on the picosecond time-scale for the nanometer-sized samples with a small number of ions. This section will discuss about the transport properties compose of mean square displacement, diffusivity and ion conductivity. The mobility of ions was characterized by these properties. Moreover, temperature effect on mobility of hydronium ion was concerned.

To imagine the movement of the ion, mean square displacement (MSD) was considered. Each consecutive step may be either forward or backward which cannot predict. In a molecular system, a molecule moves in three dimensions, but the same principle applies. Also, since the systems have many molecules to consider we can calculate a square displacement for all of them. The average square distance, taken over all molecules, gives us the mean square displacement. This is what makes the mean square displacement (MSD) significant in science: through its relation to diffusion it is a measurable quantity, one which relates directly to the underlying motion of the molecules. The linear or straight line dependence of the MSD plot is apparent. If the slope of this plot is taken, the diffusion coefficient and conductivity may be readily obtained.

2.1 Various amount of water

After running the molecular dynamics for 200 ps, all systems were analyzed by plotting the MSD versus time. Figure 12 shows the MSD ($Å^2$) of hydronium ion as a function of time (ps) for 10, 20, 30 and 40 % of water. At the same time the MSD of Cell4 is larger than the others, this means in Cell4 the hydronium ion has the longest trajectory than the others as shown in Figure 12. The MSD as a function of time was determined to get the self-diffusion coefficients of hydronium ions and water molecule in both systems from equation (4). When the time

is long enough, the diffusive regime is reached and $\langle[R_i(t)\text{-}R_i(0)]^2\rangle$ varies with time; i.e. the slope of the log $\langle[R_i(t)\text{-}R_i(0)]^2\rangle$ versus log time plots reaches unity, and the diffusion coefficient was obtained from equation (4). To check the Einstein diffusion whether or not reaching, plotting log MSD versus log time is analyzed. In Cell1 and Cell2 the slope of such curve is in the range of 0.65 - 0.75. In Cell3 and Cell4 the slope of log MSD versus log (t) curve are 0.75 – 0.85 and 0.9 – 1.0 respectively. Also DDA90, DDA80 and DDA70 correspond to Cell4. Thus the Einstein diffusion is reached in 40 % of water system only. Consequently, calculated value of 40 % of water is acceptable, but the other systems will calculate to compare trend of hydronium ion mobility. The mobility of hydronium ion in all cases slightly increases when the amount of water in the system increases.

The MSD as a function of time was determined to get the self-diffusion coefficients of ions from equation (4). In cell4 the Einstein diffusion was reached for the hydronium ion in all cases. The diffusion coefficient of the hydronium ion is 5.5×10^{-11} m^2/s in Cell1, 0.072×10^{-9} m^2/s in Cell2, 0.182×10^{-9} m^2/s in Cell3 and 0.32×10^{-9} m^2/s in Cell4. This indicates that diffusivity of the ion increases as the amount of water increases (Figure 13). The diffusion coefficient of water is 0.34×10^{-9} m^2/s for Cell1 0.61×10^{-9} m^2/s in Cell2, 1.36×10^{-9} m^2/s in Cell3 and 1.74×10^{-9} m^2/s for Cell4. The value of ion conductivity calculated by using equation (5) for Cell4 is 7.14×10^{-2} S/cm (see Appendix B). This value was compared with the experimental work of Wan *et al*. (2003). The values that they have found were as high as $10^{-5} – 10^{-3}$ S/cm for hydrated membrane. Mukoma *et al.* (2004) found the conductivity of chitosan was 5×10^{-3} S/cm. The corresponding method and result of López-Chávez *et al*. (2005) were compared with this result. They suggest that the percent of water and sulfates may improve the ion conductivity in chitosan membranes until a value of 2×10^{-2} S/cm. Ennari (2008) work obtained the conductivity of sulfonated PVF – base materials. The value of conductivity is $(91\pm9) \times 10^{-3}$ S/cm in 40 % of water system. Such information was calculated for 298 K only, for the others were concluded as Table 3. As a conclusion, the diffusivity and ion conductivity increase as amount of water in the system increases. The reason why the diffusivity of hydronium ion

increases according to the numbers of water in the system will discuss in the section 3.1 (coordination study).

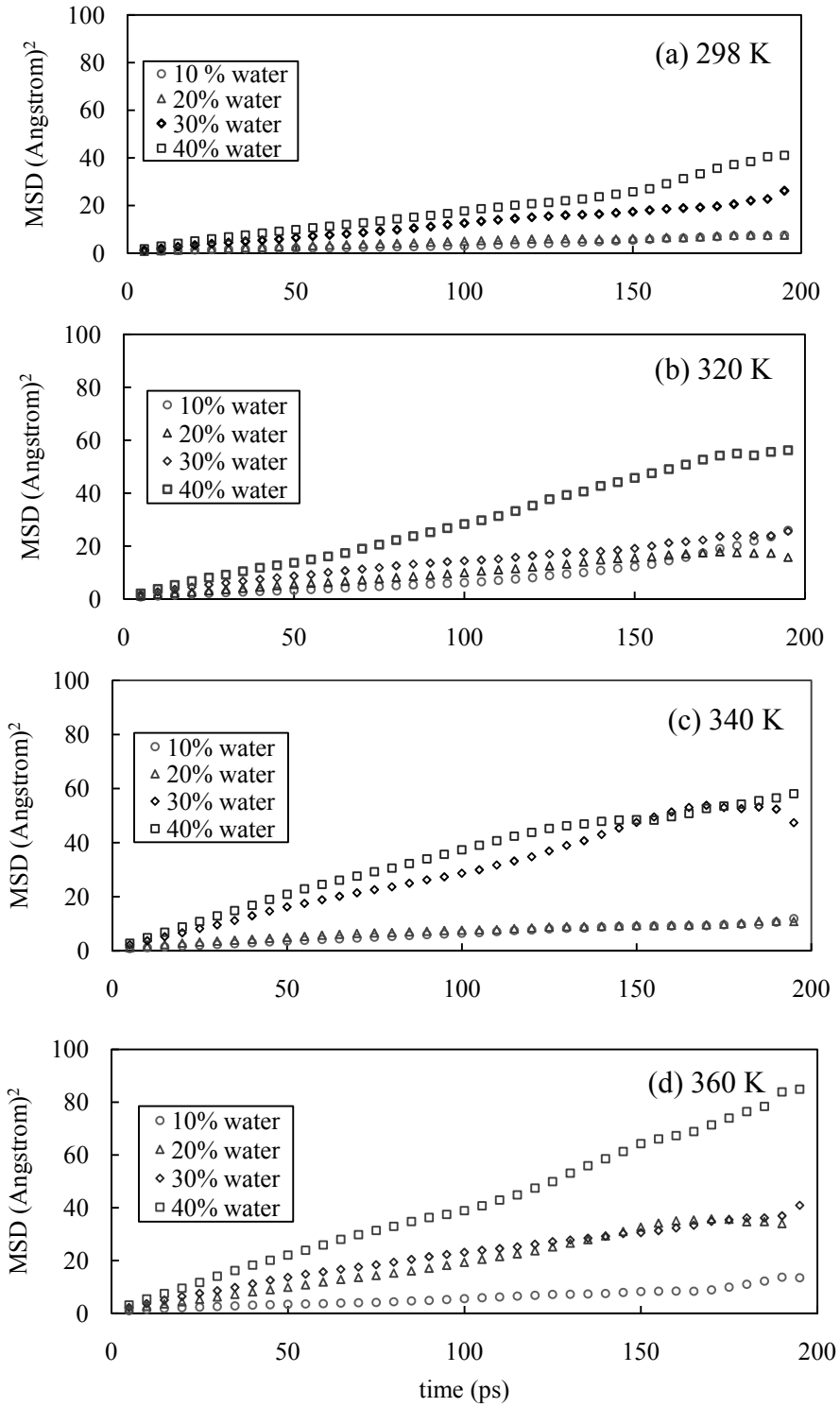

Figure 12 Mean square displacement of hydronium ion as a function of time at 298 K (a), 320 K (b), 340 K (c) and 360 K (d).

Table 3 The diffusivity and the ion conductivity for all systems at various temperatures.

system	Diffusion coefficient (m^2/s)	Ion conductivity (S/cm)
298 K		
Cell1	0.055×10^{-9}	0.0134
Cell2	0.072×10^{-9}	0.0156
Cell3	0.182×10^{-9}	0.0338
Cell4	0.32×10^{-9}	0.0714
DDA90	0.71×10^{-9}	0.112
DDA80	0.49×10^{-9}	0.0756
DDA70	0.58×10^{-9}	0.088
320 K		
Cell1	0.118×10^{-9}	0.0266
Cell2	0.162×10^{-9}	0.0322
Cell3	0.192×10^{-9}	0.0332
Cell4	0.495×10^{-9}	0.074
340 K		
Cell1	0.0967×10^{-9}	0.0204
Cell2	0.090×10^{-9}	0.0168
Cell3	0.475×10^{-9}	0.0774
Cell4	0.581×10^{-9}	0.0818
360 K		
Cell1	0.078×10^{-9}	0.0156
Cell2	0.34×10^{-9}	0.0594
Cell3	0.31×10^{-9}	0.048
Cell4	0.69×10^{-9}	0.0926

Note: Cell1 (10 % of water), Cell2 (20 % of water), Cell3 (30 % of water), Cell4 (40 % of water)

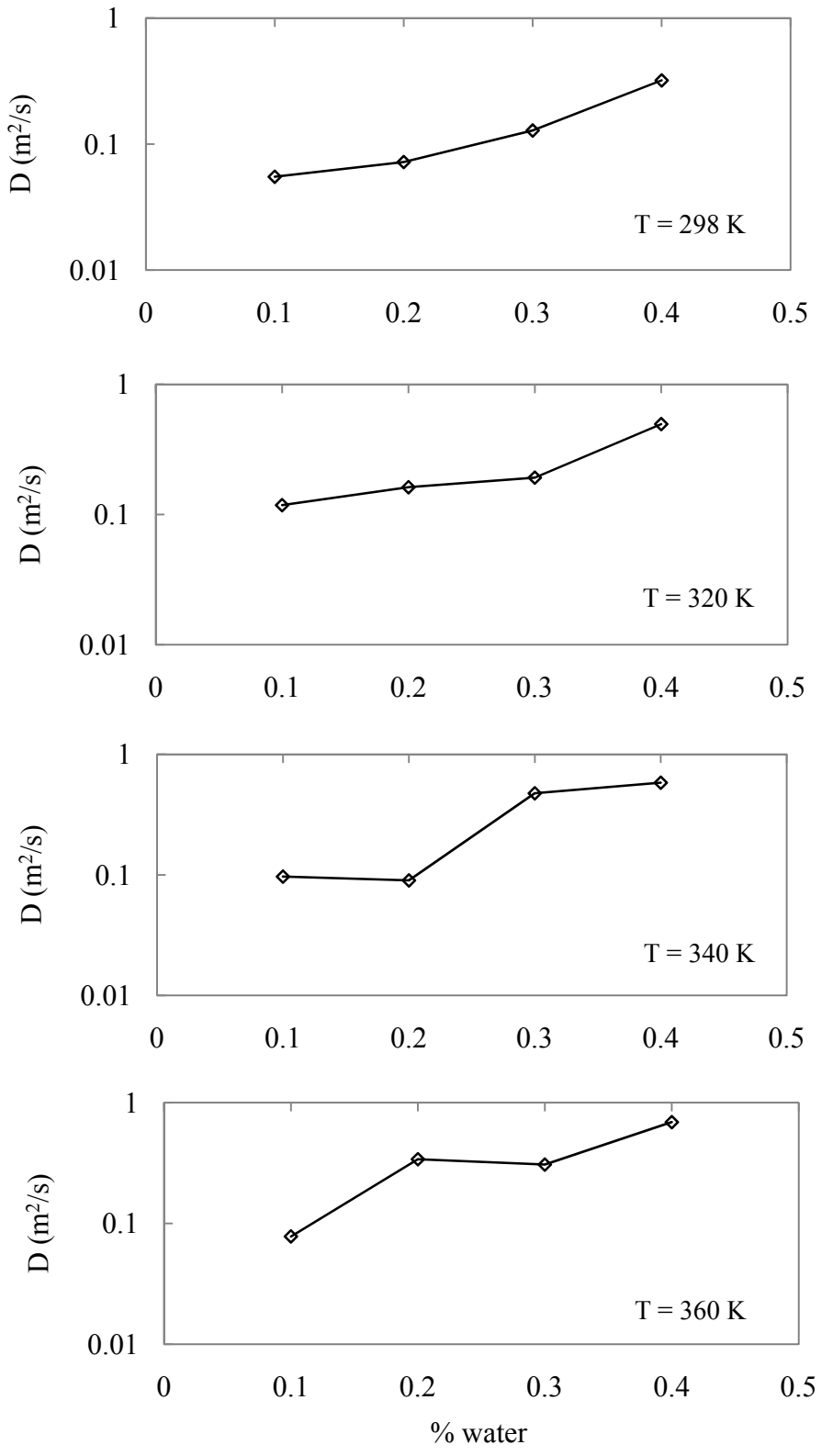

Figure 13 The diffusion coefficients of hydronium ion with different temperatures.

2.2 Temperature effect

The dynamical property was studied in the temperature range of 298 – 360 K. The temperature effect on conductivity was considered. The condition of PEM was operated in the range 298 – 360 K and various amounts of water. After considering each system, as temperature is increased the diffusivity is slightly changed. Nevertheless, the temperature is fixed at the same certain value, the diffusivity still increase according to the numbers of water in the system increase as shown in Figure 13.

In Cell4 Einstein diffusion was reached for ions, which means that their motion is uncorrelated with their motion at any privious time and that Einstein equation is valid. Thus the value of conductivity could be calculated for this system. The ion conductivity is 0.0714 S/cm at 298 K, 0.074 S/cm at 320 K, 0.0818 S/cm at 340 K and 0.0926 S/cm at 360 K. The temperature dependence of the conductivity in Figure 14 shows that this parameter for hydronium ion also follows Arrhenius behavior. This means the conductivity increases as the temperature increases. Figure 14a shows the standard electrolyte materials for low and high temperature fuel cells (Kreuer *et al*., 2004) and quite a few old and new materials have been reported that show interesting conductivities, especially in the intermediate temperature range. Chitosan membrane with 40 wt% of water in Figure 14 placed in Figure 14a. The conductivity data of chitosan was used for developing proton exchange membrane.

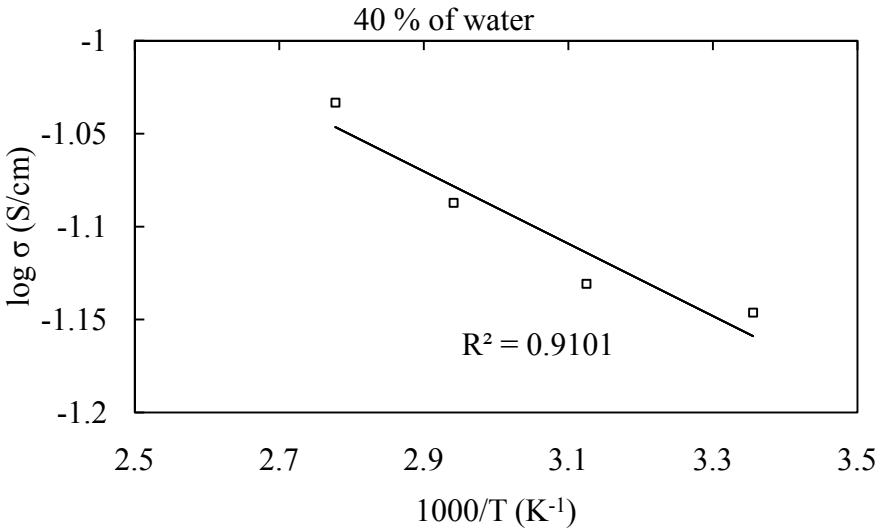

Figure 14 The ion conductivity of chitosan membrane in Cell4 at different temperatures.

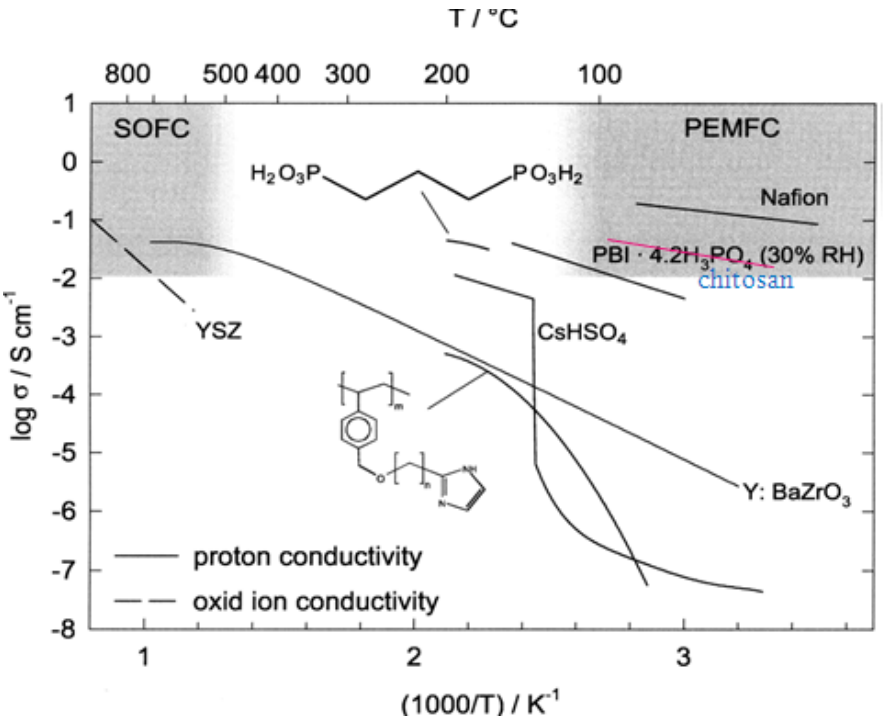

Figure 14a Conductivity of some intermediate-temperature proton conductors, compared to the conductivity of Nafion and the oxide ion conductivity of YSZ (yttria- stabilized zicronia), the standard electrolyte materials for low and high temperature fuel cells, proton exchange membrane fuel cell (PEMFCs), and solid oxide fuel cells (SOFCs).

Source: Kreuer *et al*. (2004)

2.3 Various degree of deacetylation (DDA)

The disscussions for the DDA system shown in Table 3, the diffusivity and conductivity are slightly higher than Cell4, due to the number of water molecule little higher to keep 40 weight % of water in all system. From Table 3, the ion conductivity of Cell4, DDA90, DDA80 and DDA70 are 0.0714, 0.112, 0.0756, and 0.088 S/cm, respectively (Figure 15). The computational values are not follow the experimental work of Wan *et al*. (2003). In real materials, they do that the DDA (70-92%) of chitosan affects slightly the conductivity of membrane divided in two cases, hydrated membrane and dry membrane. The conductivity increases as the DDA increases for dry membrane, while the conductivity is slightly decreased as the DDA increases for hydrate menbrane. In this study, the DDA systems (70-100%) which have 40 % of water contained were compared to hydrate membrane of Wan *et al*. (2003). It was found that computational values are different from experimental trend. However, this unfitting results due to this technique calculation from the diffussion.

The higher content of amino groups in chitosan membranes may contribute a higher ionic conductivity, because of the amino group in chitosan backbone are partially protonated ($NH_2 + H_2O \leftrightarrow NH_3^+ + OH^-$ or $NH_2 + H_3O^+ \leftrightarrow NH_3^+ + H_2O$) also proton transfer mechanism will occurred. This is the idea for ion transfer mechanism. Thus, conductivity should be increase as the amino group of chitosan. However, this contrasting between the idea and the results for hydrated membrane was considered in the next section (section 3.2).

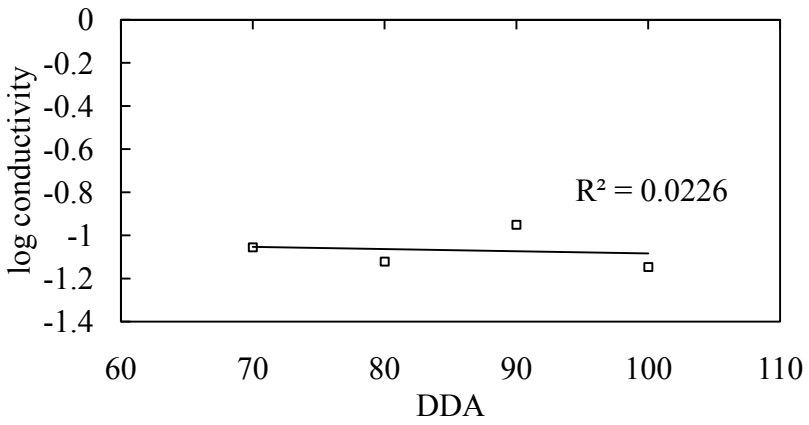

Figure 15 Ionic conductivity of chitosan membranes with varied DDA, 40 % water.

3. Coordination study

This section will discuss concerning the location of hydronium ion and water molecule with functional group of chitosan, amino group ($-NH_2$), hydroxyl group (-OH), methoxyl group ($-CH_2OH$) and acetyl group ($-COCH_3$). When the amount of water increases, the functional groups of chitosan have significant. The coordination between the particles in the systems was studied by calculating the intermolecular pair correlation functions between the particles. Especially the coordination of the hydronium ion was studied to get information of the mechanism of conductivity. The coordination was studied by plotting the pair correlation function *g(r)* as a function of the separation distance *r*.

3.1 Coordination between chitosan and hydronium ion or water molecule for system with various amounts of water

The pair correlation function between the oxygen atom in the hydronium ion and the nitrogen atom in the amino group of chitosan chain is shown in Figure 16. For short distances, *g(r)* is zeros. This is due to the strong repulsive forces. The first and largest peak occurs at 2.75 Å due to the first coordination shell. The curves of the pair correlation function for Cell1, Cell2, Cell3 and Cell4 are similarly. The coordination number was calculated from these curves (see Appendix C). The

coordination number was 0.72 in Cell1**,** while it is 0.70 in Cell2, 0.48 in Cell3 and 0.38 in Cell4. The number of the hydronium ions is the same (20 ions) in Cell1, Cell2, Cell3 and Cell4. Thus, the coordination between hydronium ion and the amino group in chitosan chain decreases as the number of water in the system increases. The pair correlation function between the oxygen atom in the water molecule and the nitrogen atom in the amino group of chitosan chain is shown in Figure 16. The maximum peak is found in the broad range 2.8-3.5 Å. The coordination number is 0.59 in Cell1, while it is 1.10 in Cell2, 1.34 in Cell3 and 1.91 in Cell4. Thus, the coordination between water molecule and the amino group of chitosan chain increases with the number of water in the system increase. As a conclusion, it can be seen that the coordination between the amino group of chitosan and the hydronium ion decreases with increasing amount of water.

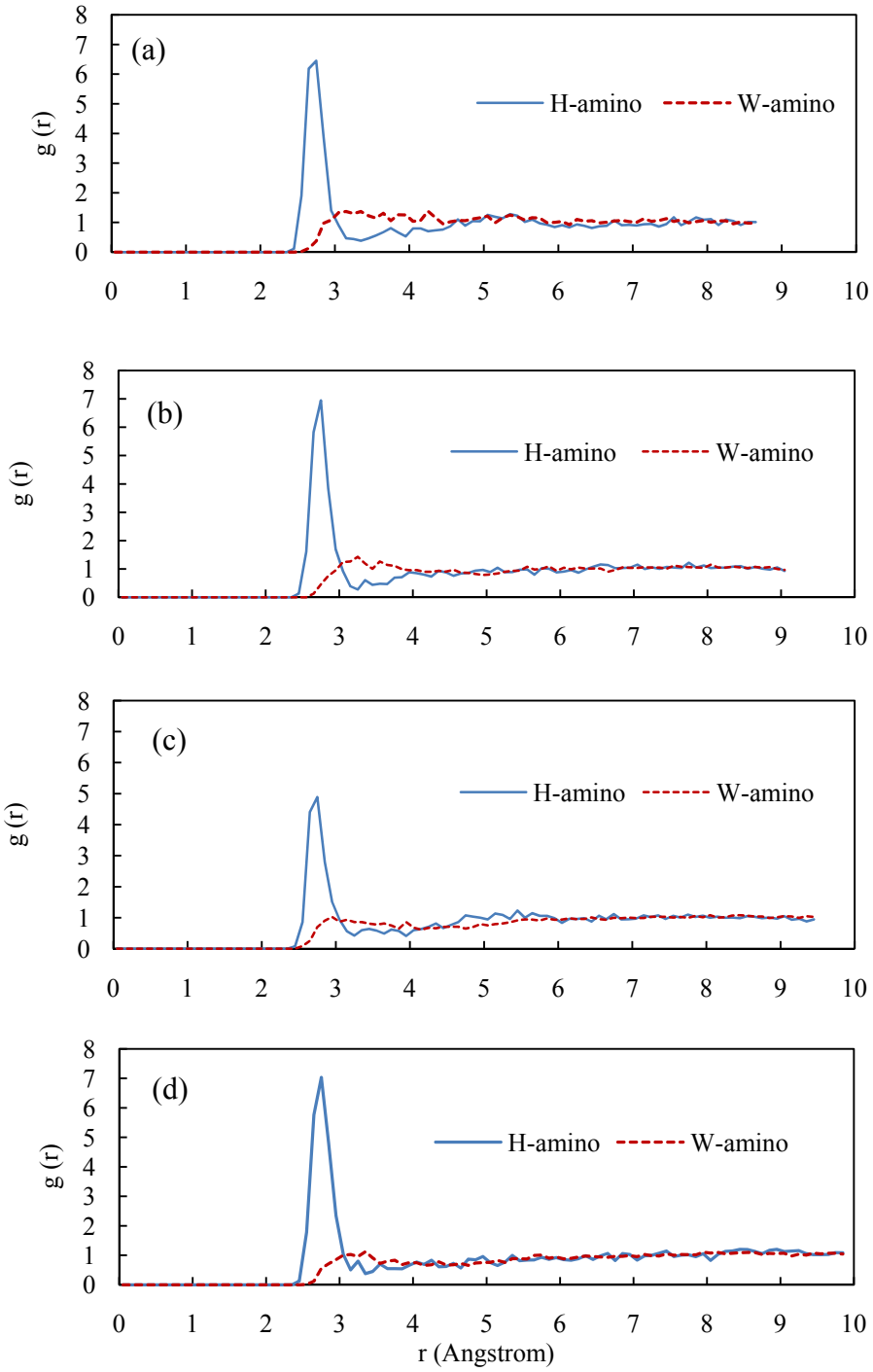

Figure 16 The pair correlation function between the oxygen atom in the hydronium ion and the nitrogen atom in the amino group of chitosan chain (H_3O^+---NH_2-) and between the oxygen atom in the water molecule and the nitrogen atom in the amino group of chitosan chain (H_2O---NH_2-) in Cell1 (a), Cell2 (b), Cell3 (c) and Cell4 (d).

The second functional group, hydroxyl group (-OH) is considered. The pair correlation function between the oxygen atom in the hydronium ion and the oxygen atom in hydroxyl group of chitosan chain is shown in Fgure 17. The first coordination shell is found at 2.55 Å. The coordination number is 0.72 in Cell1, while it is 0.49 in Cell2, 0.39 in Cell3 and 0.28 in Cell4. The largest number of hydronium ion appears in small amount of water (10 % of water). The coordination between hydronium ion and hydroxyl group is decreased driving an increasing of number of water. The pair correlation function between the oxygen atom in the water molecule and the oxygen atom in hydroxyl group of chitosan chain is shown in Figure 17. The first coordination shell is found at 2.75 Å. The coordination number is 0.70 in Cell1, while it is 1.14 in Cell2, 1.10 in Cell3 and 1.48 in Cell 4. Thus, the coordination between water molecule and the hydroxyl group of chitosan chain slightly increases with the number of water in the system. However, the position of hydronium ions is shorter than water molecules. This due to the hydronium ions located around amino group. The coordination numbers of water molecule located around the hydroxyl group are slightly higher than the hydronium ions. As a conclusion, the hydronium ions are more strongly coordinated to the hydroxyl group in Cell1 than the others, while in Cell4 they can better transfer to water site.

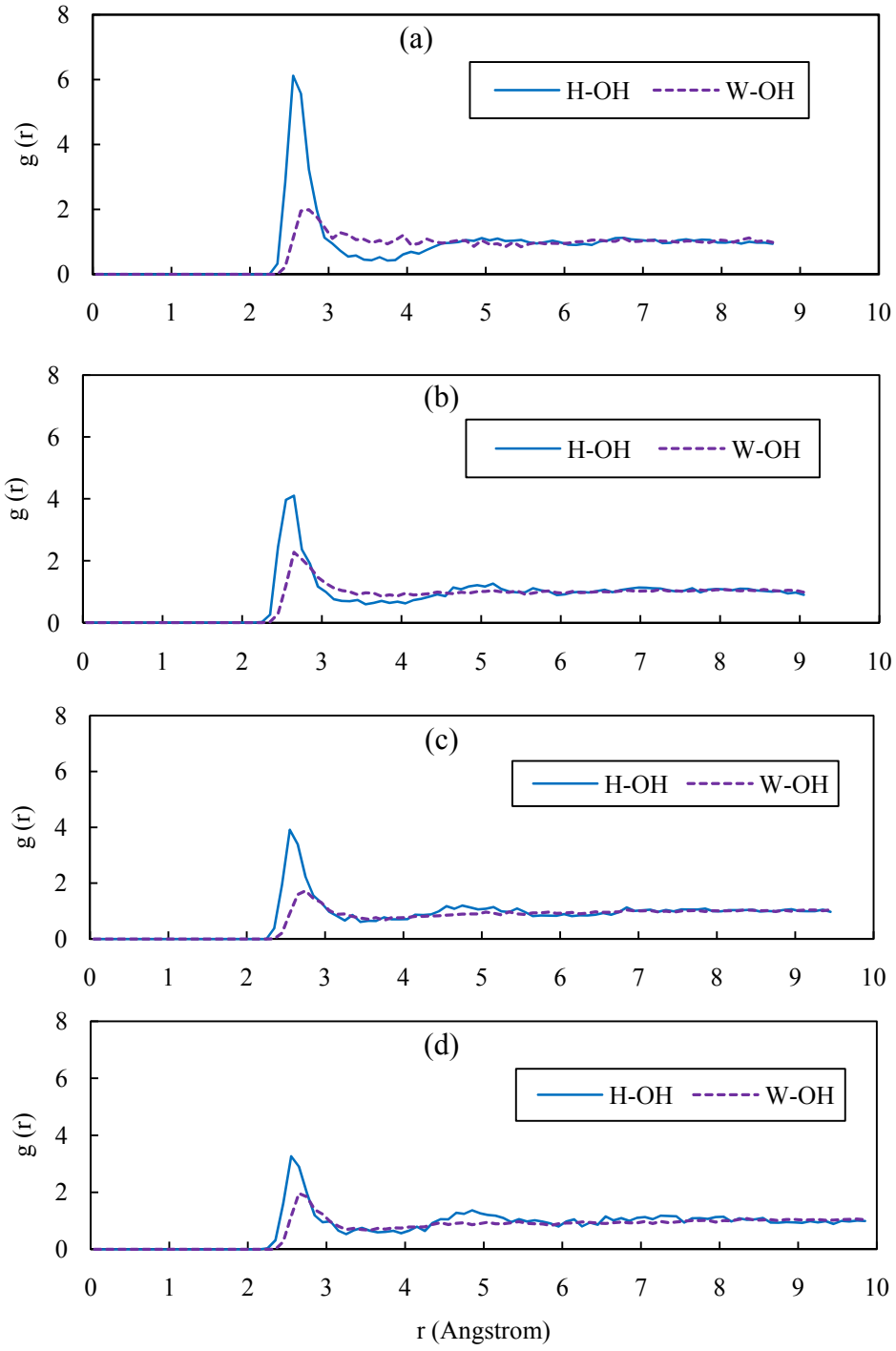

Figure 17 Pair coorelation function between the oxygen atom in the hydronium ion and the oxygen atom in hydroxyl group of chitosan chain (H_3O^+---OH) and between the oxygen atom in the water molecule and the oxygen atom in hydroxyl group of chitosan chain (H_2O---OH) in Cell1 (a), Cell2 (b), Cell3 (c) and Cell4 (d).

The third functional group, methoxyl group (-CH_2OH) is considered. The pair correlation function between the oxygen atom in the hydronium ion and the carbon atom in methoxyl group of chitosan chain is shown in Fgure 18. The first coordination shell is found at 3.55 Å. The coordination number is 1.17 in Cell1, while it is 0.93 in Cell2, 0.64 in Cell3 and 0.48 in Cell4. The coordination between hydronium ion and methoxyl group is decreased driving an increasing of number of water. It can be seen that hydronium ions are more strongly coordinated to methoxyl group in Cell1 than the others. The pair correlation function between the oxygen atom in the water molecule and the carbon atom in methoxyl group of chitosan chain is shown in Figure 18. The first coordination shell is found at 3.55 Å which the same position as the hydronium ion. The coordination number is 1.20 in Cell1, while it is 2.26 in Cell2, 2.66 in Cell3 and 3.25 in Cell 4. Thus, the coordination between water molecule and the methoxyl group of chitosan chain increases with the number of water in the system. However, the position of hydronium ions and water molecules are the same, but coordination number of water molecule located around the methoxyl group are larger than the hydronium ions. When the number of water increases, hydronium ions are not mainly located around the functional group of chitosan and especially in Cell4 they are elsewhere.

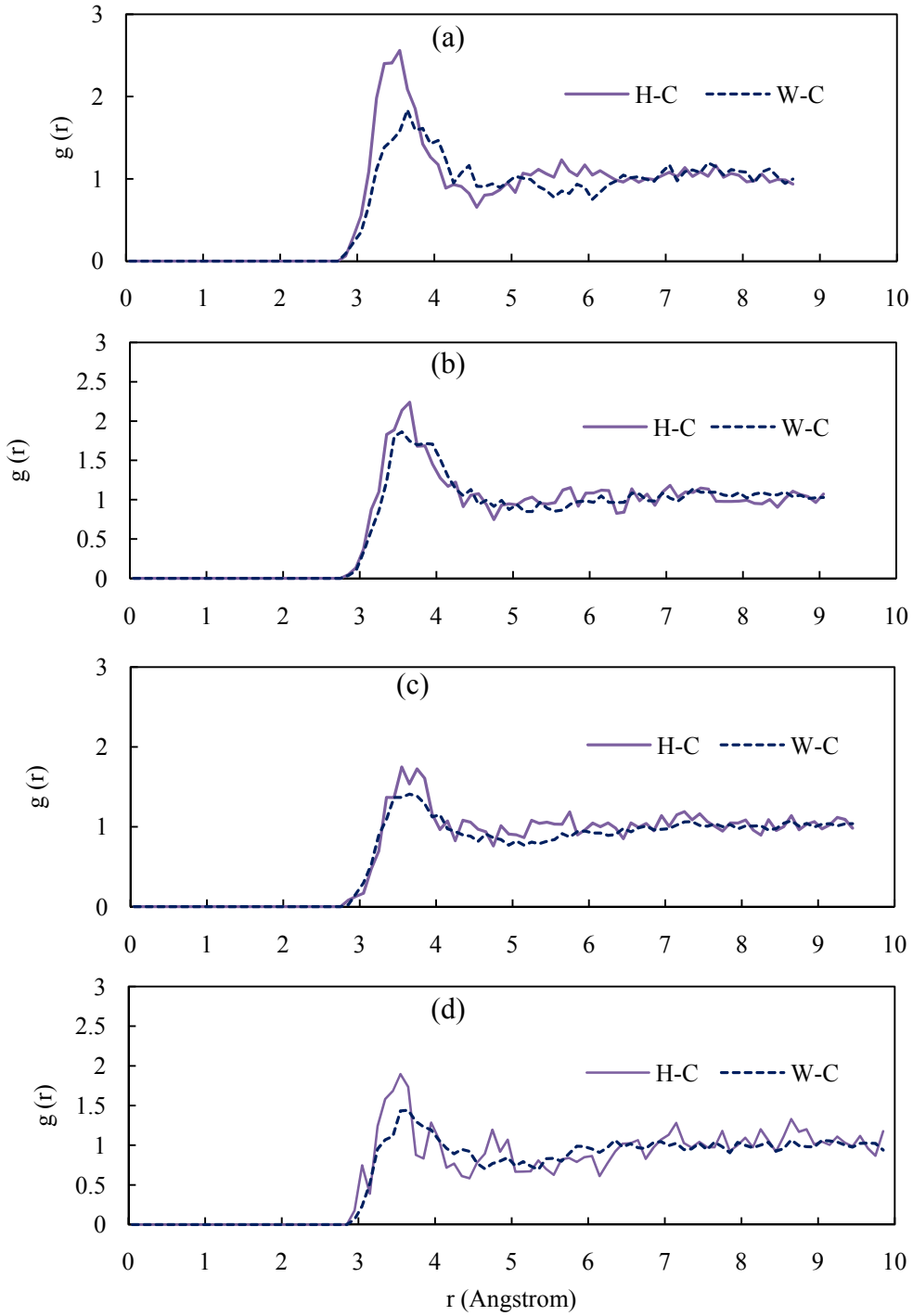

Figure 18 The pair correlation function between the oxygen atom in the hydronium ion and the carbon atom in methoxyl group of chitosan chain (H_3O^+---CH_2OH) and between the oxygen atom in the water molecule and the carbon atom in methoxyl group of chitosan chain (H_2O---CH_2OH) in Cell1 (a), Cell2 (b), Cell3 (c) and Cell4 (d).

The pair correlation function between the oxygen atom in the hydronium ion and the oxygen atom in water molecule is shown in Figure 19. The shapes of curve are the same for all system and the same position of the first coordination shell at 2.55 Å. This position is also in agreement with Ennari (2008), 2.6 Å. The coordination number in the first coordination shell is 1.06 in Cell1, while it is 1.34 in Cell2, 2.63 in Cell3 and 3.16 in Cell4. This means that coordination between hydronium ion and water molecule increase as amount of water in the system increase. The pair correlation function between oxygen atoms in hydronium ion is shown in Figure 19. The shapes of curve are the same for all systems and the same position of the first coordination shell in range of 4.45 - 4.65 Å which is the same position of second coordination shell between hydronium and water. The coordination number in the first coordination shell is 1.69 in Cell1, while it is 1.41 in Cell2, 1.22 in Cell3 and 1.09 in Cell4. This indicates that there is no interaction between hydroniun ions. The pair correlation function between oxygen atoms in water molecule is shown in Figure 19. There is a strong peak at 2.75 Å with coordination number 0.87 in Cell1, 2.02 in Cell2, 2.92 in Cell3 and 3.58 in Cell4. The location of hydronium ion and water molecule are important. Coordination number between hydronium ion and water molecule is 3, there are 3 molecules of water located around hydronium ion or eigen structure is formed in Cell4. Coordination number between water molecules is about 4, there are 4 molecules of water located around one water molecule or water cluster is formed in Cell4.

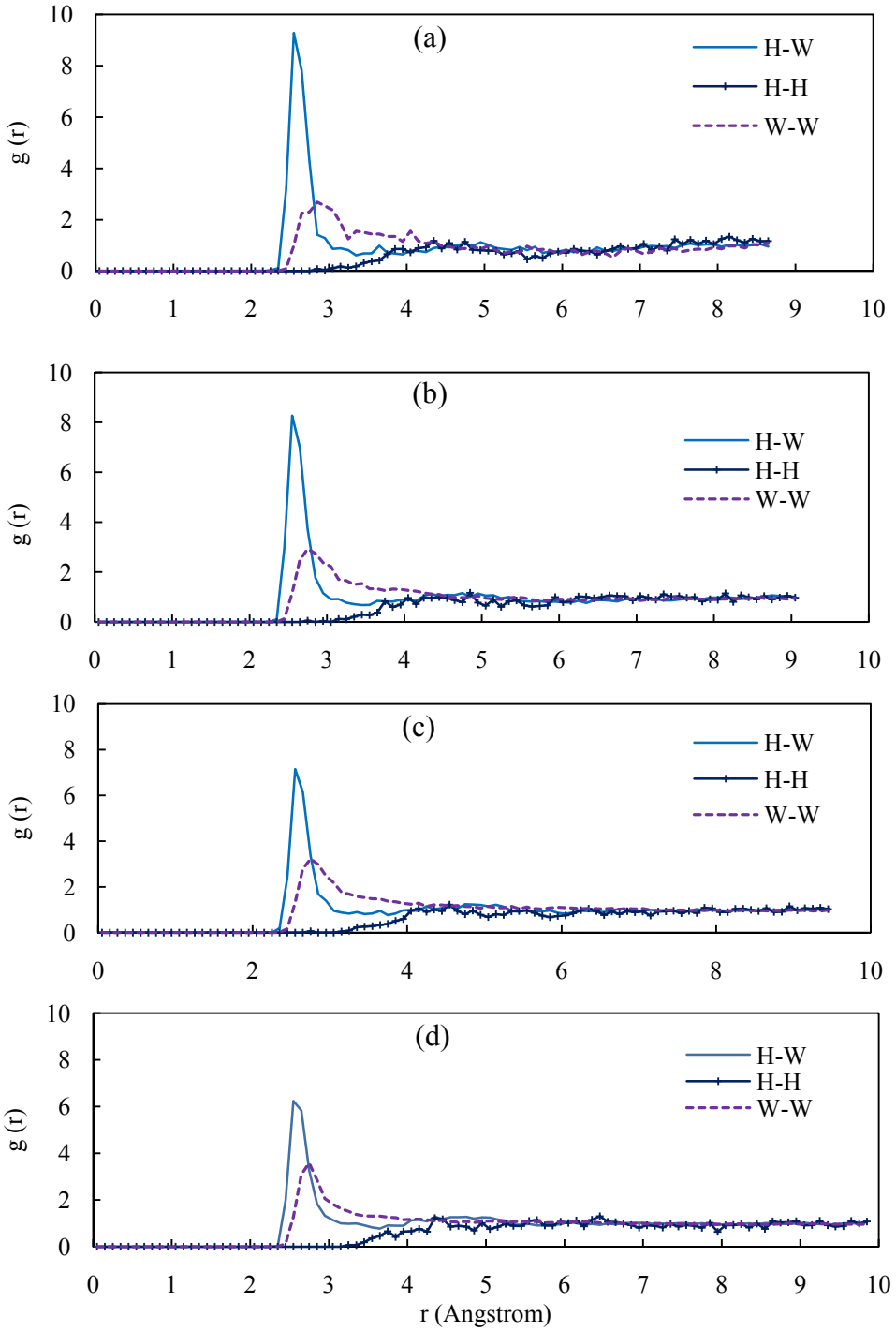

Figure 19 The pair correlation function between the oxygen atom in the hydronium ion and the oxygen atom in water molecule in Cell1 (a), Cell2 (b), Cell3 (c) and Cell4 (d).

When we consider each system; for example in Cell4, the pair correlation between the hydronium ion and the amino group are shown in Figure 16. The strong coordination shell is found at 2.75 Å with coordination number is 0.38. Pair correlation between the water and the amino group show the first peak at 3.05 Å with coordination number 1.91. Pair correlation function between hydronium or water and hydroxyl group of chitosan illustrated in Figure 17. The first peak of hydronium ion appeared at 2.55 Å with coordination number 0.28. The distance between water molecule and hydroxyl group is 2.75 Å and coordination number 1.48. The pair correlation function between the hidronium ion or water molecule and the methoxyl group of chitosan chain are shown in Figure 18. The former show the first peak at 3.55 Å with coordination number was 0.48 and the latter show the first peak at 3.55 Å with coordination number was 3.25. Pair correlation function between the hydronium ion and the water molecule show the strong peak at 2.55 Å with the coordination number 3.16 as shown in Figure 19. Such information indicated that the length between hydronium ion and amino group is shorter than the water molecule which located around amino group. This hydronium ion is located close to hydroxyl group. Hydronium ion and water molecule which located around the methoxyl group are the same length. The coordination between water and hydronim ion is 3. Therefore, the eigen ion is formed. Such information indicated that hydronium ions are not mainly located around the backbone or functional group of chitosan, but they form eigen ion which makes to obtain the diffusivity in 40 % of water system. Moreover, function groups of chitosan are more absorbability of water.

3.2 Coordination between chitosan and hydronium ion or water molecule for system with various DDA

In the DDA system (40 % of water), the pair correlation function between the oxygen atom in the hydronium ion and the nitrogen atom in the amino group of chitosan chain is shown in Figure 20. There is a strong peak at 2.75 Å due to the first coordination shell. The curves of the pair correlation function for DDA90, DDA80 and DDA70 are similarly. The coordination number was calculated from these curves. The coordination number is 0.57 in DDA90**,** while it is 0.36 in DDA80 and 0.45 in DDA70. The number of water in DDA system is high as 40 wt% of water system.

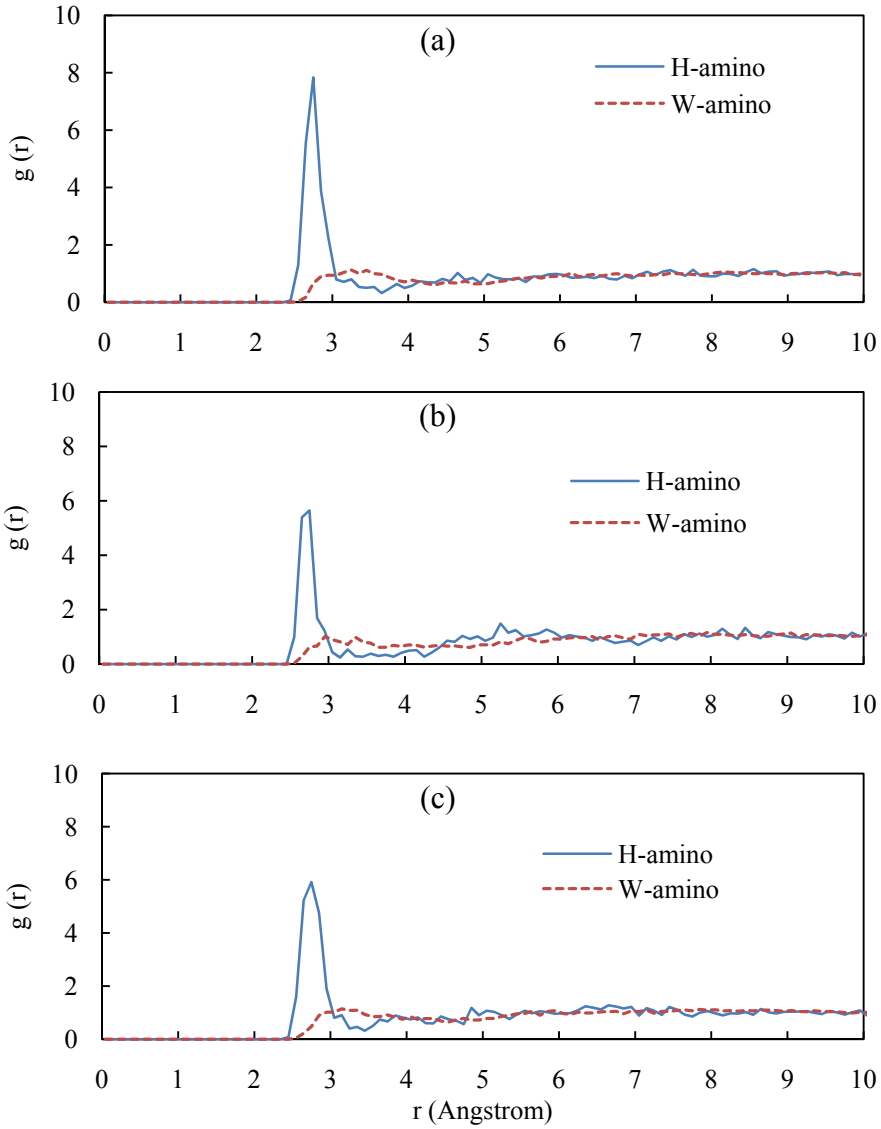

Figure 20 The pair correlation function between the oxygen atom in the hydronium ion and the nitrogen atom in the amino group of chitosan chain (H_3O^+---NH_2-) and between the oxygen atom in the water molecule and the nitrogen atom in the amino group of chitosan chain (H_2O---NH_2-) in DDA90 (a), DDA80 (b) and DDA70 (c) systems.

The pair correlation function between the oxygen atom in the water molecule and the nitrogen atom in the amino group of chitosan chain is refered from Figure 16. The maximum peak appeared in the broad range 2.8-3.5 Å. The coordination number of DDA90, DDA80 and DDA70 are 1.96, 1.91 and 1.92, respectively. It can be indicated that the coordination between water molecule and the

amino group of chitosan chain is about the same because of its identical numbers of water.

The pair correlation function between the oxygen atom in the hydronium ion and the oxygen atom in hydroxyl group of chitosan chain is shown in Fgure 21. The first coordination shell is found at 2.55 Å. The coordination number is 0.32, 0.27 and 0.28 in DDA90, DDA80 and DDA70 respectively. The pair correlation function between the oxygen atom in the water molecule and the oxygen atom in hydroxyl group of chitosan chain is shown in Figure 20. The first coordination shell is found at 2.75 Å which the same position as the hydronium ion. The coordination number is 1.38 in DDA90, while it is 1.49 in DDA80 and 1.32 in DDA70. This information corresponded to Cell4. Thus it seems that hydronium ions are not mainly located around the hydroxyl group of chitosan and water molecule located there about 1 molecule.

The pair correlation function between the oxygen atom in the hydronium ion and the carbon atom in methoxyl group of chitosan chain in DDA systems are shown in Fgure 22. The first coordination shell is found at 3.55 Å for. The coordination number is 0.5 in DDA90, while it is 0.5 in DDA80 and 0.55 in DDA70. The coordination between hydronium ion and methoxyl group are the same in DDA systems. The pair correlation function between the oxygen atom in the water molecule and the carbon atom in methoxyl group of chitosan chain is shown in Figure 22. The first coordination shell is found at 3.55 Å which the same position as the hydronium ion. The coordination number is 3.19 in DDA90, while it is 3.36 in DDA80 and 3.79 in DDA70. Thus, the coordination between water molecule and the methoxyl group of chitosan chain is not different. However, the position of hydronium ions and water molecules are the same but coordination number of water molecule located around the methoxyl group are larger than the hydronium ions. Such position is not has significant for the conductivity. It can be seen that hydronium ions are not mainly located around the methoxyl group of chitosan and water molecule located there about 3 molecules.

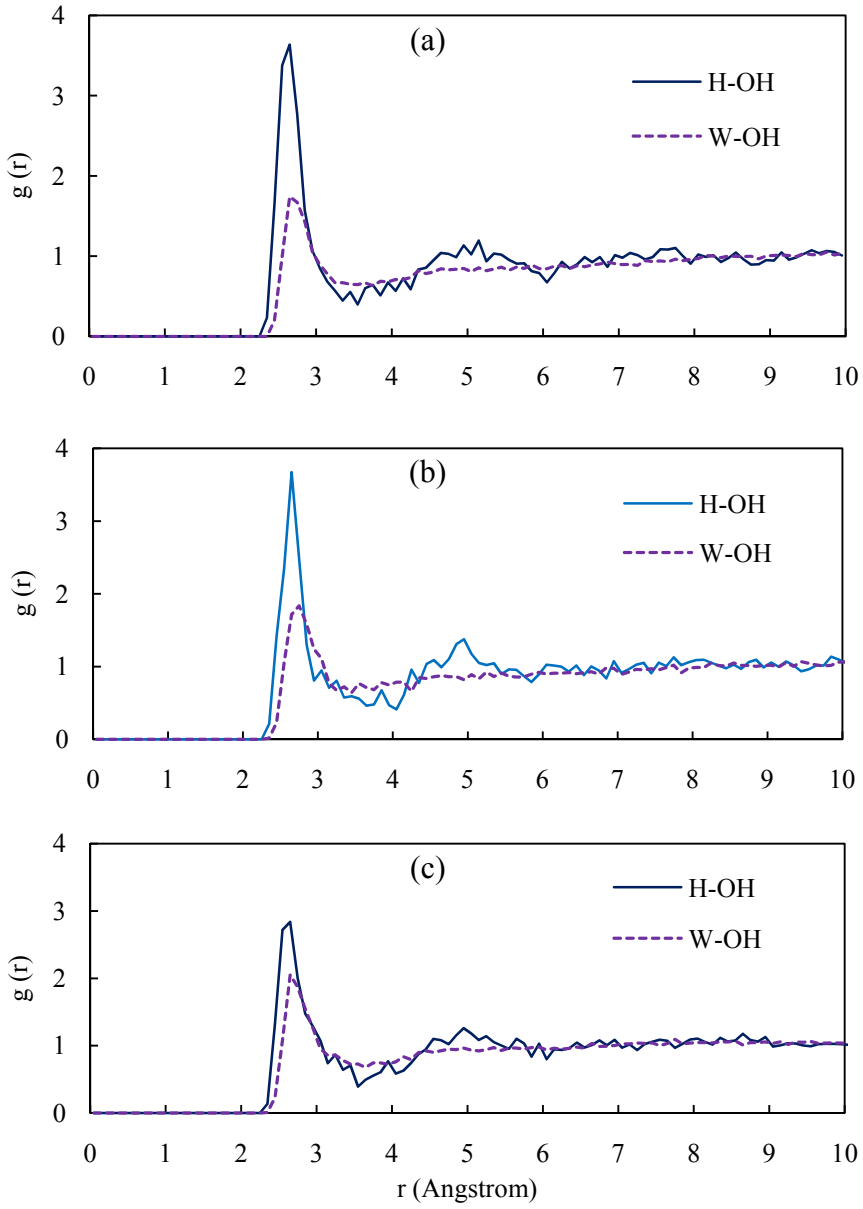

Figure 21 The pair correlation function between the oxygen atom in the hydronium ion and the oxygen atom in the methoxyl group of chitosan chain (H_3O^+---OH) and between the oxygen atom in the water molecule and the oxygen atom in the methoxyl group of chitosan chain (H_2O---OH) in DDA90 (a), DDA80 (b) and DDA70 (c) system.

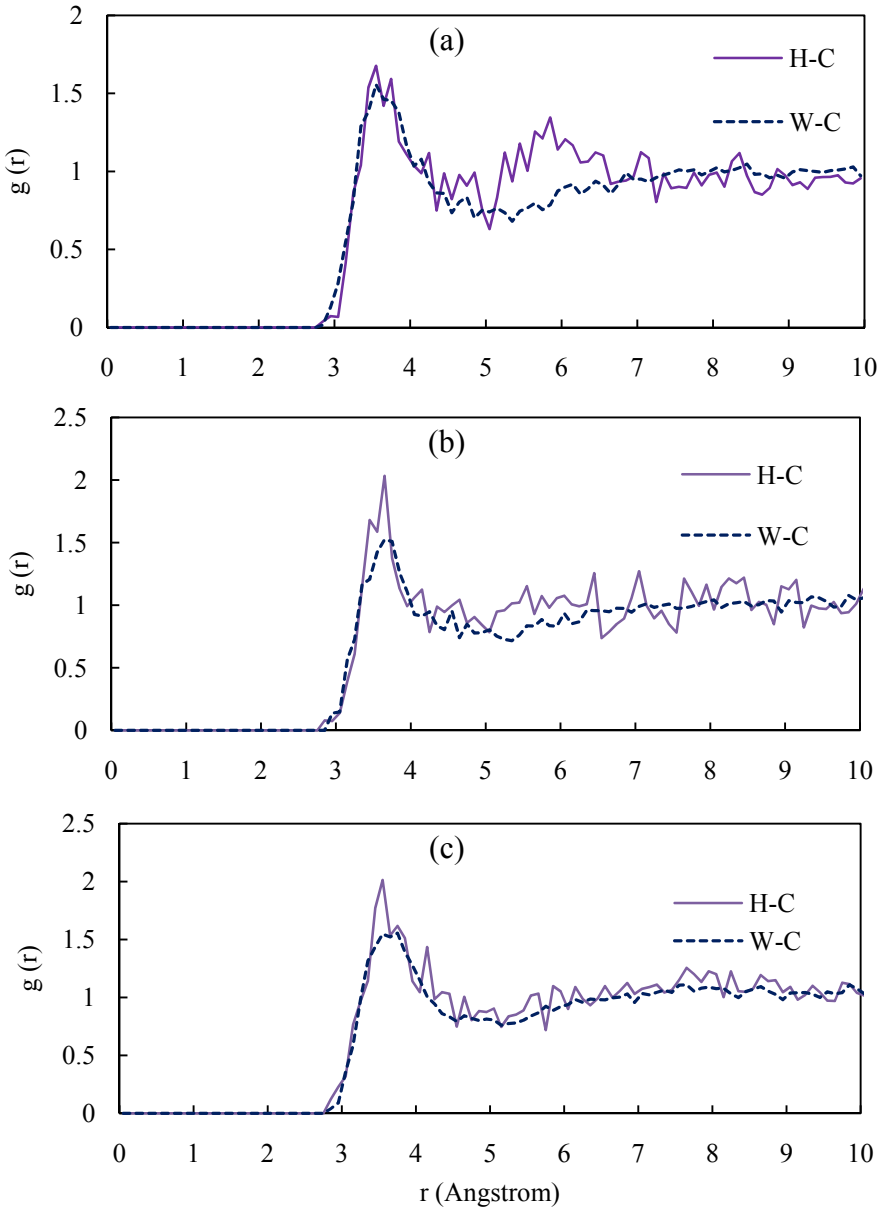

Figure 22 The pair correlation function between the oxygen atom in the hydronium ion and the carbon atom in methoxyl group of chitosan chain (H_3O^+---CH_2OH) and between the oxygen atom in the water molecule and the carbon atom in methoxyl group of chitosan chain (H_2O---CH_2OH) in DDA90 (a), DDA80 (b) and DDA70 (c) system.

The pair correlation function between the oxygen atom in the hydronium ion and the oxygen atom in acetyl group of chitosan chain in DDA systems are also studied (Fgure 23). The first coordination shell is found at 2.85 Å for DDA80 and DDA70. The first peak of coordination shell of DDA90 system is found at 3.25 Å. DDA90 has only one acetyl group, thus the probability of finding pair of hydronium ion and acetyl group is least. The coordination number is 0.02 in DDA90, while it is 0.06 in DDA80 and 0.4 in DDA70. The coordination between hydronium ion and acetyl group are increased with acetyl group in DDA systems increase. The pair correlation function between the oxygen atom in the water molecule and the oxygen atom in acetyl group of chitosan chain is shown in Figure 23. The first coordination shell is found at 2.85 Å which the same position as the hydronium ion. The coordination number is 1.84 in DDA90, while it is 1.71 in DDA80 and 1.89 in DDA70. Thus, the coordination between water molecule and the acetyl group of chitosan chain is not different. However, the position of hydronium ions and water molecules are the same but coordination number of water molecule located around the acetyl group are larger than the hydronium ions. Such position is near the length between hydronium or water and amino group. The acetyl group has no effect for the conductivity for this method, but in experimental work of Wan *et al.* (2003) found that the conductivity was slightly decreased when the degree of deacetylation was high for hydrated membrane, contrast with the idea of proton transfer mechanism. They found that conductivities were the same order of magnitude of 10^{-4} S/cm for the various DDA of 70-92 %, while the computational results of conductivities are 10^{-2} S/cm for 70-100 % of DDA.

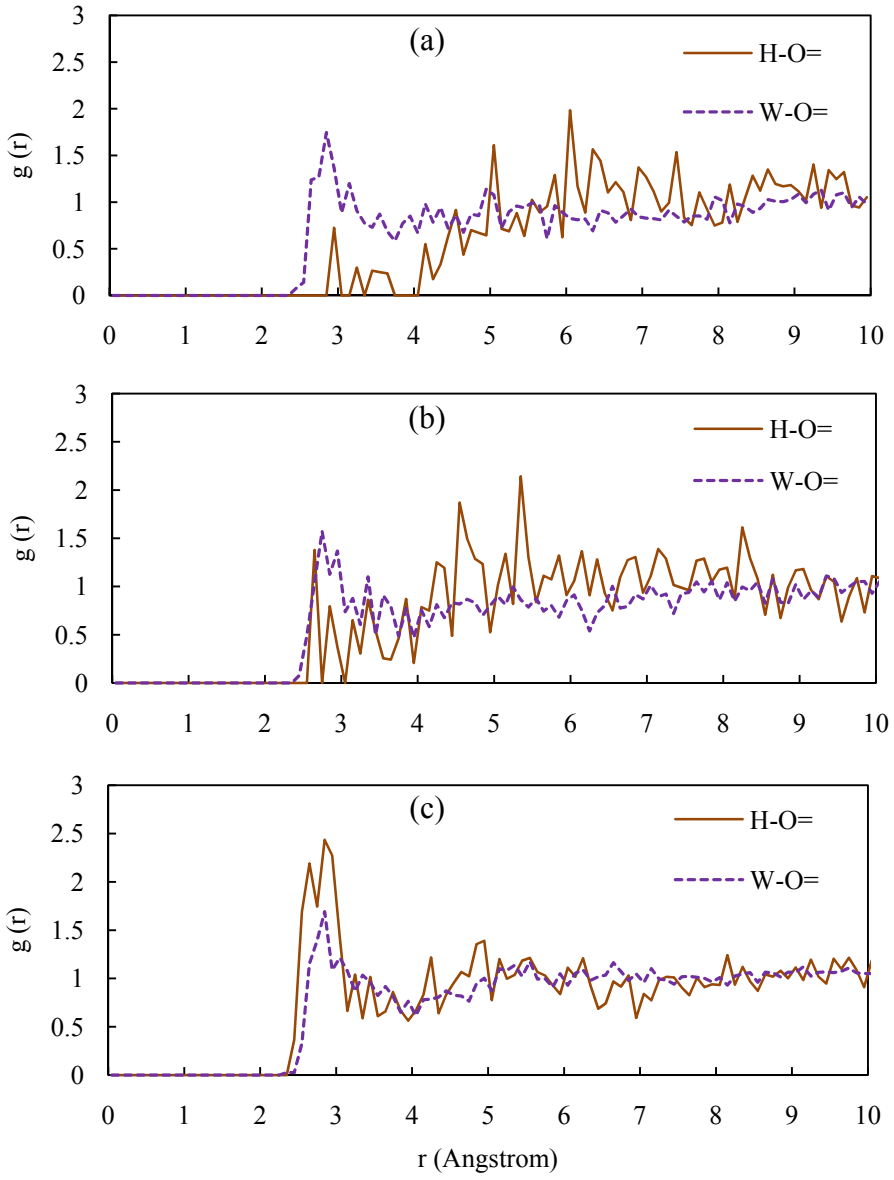

Figure 23 The pair correlation function between the oxygen atom in the hydronium ion and the oxygen atom in the acetyl group of chitosan chain (H_3O^+---O=C) and between the oxygen atom in the water molecule and the oxygen atom in the acetyl group of chitosan chain (H_2O---O=C) in DDA90 (a), DDA80 (b) and DDA70 (c) system.

The location of hydronium ions and water molecules in the system was considered. The pair correlation function between the oxygen atom in the hydronium ion and the oxygen atom in water molecule is shown in Figure 24. The shapes of curve are the same for all system and the same position of the first coordination shell at 2.55 Å. This position is also in agreement with Ennari (2008), the distance between oxygen atom in the hydronium ion and the oxygen atom in water is reported to be 2.6 Å. The coordination number in the first coordination shell is 3.35 in DDA90, while it is 3.22 in DDA80 and 3.12 in DDA70, which the eigen ion ($H_9O_4^+$) is formed. The second coordination shell is at 4.75 Å with coordination number is 7.0 in DDA90 and 6.8 in DDA80 and 6.7 in DDA70. This means that coordination between hydronium ion and water molecule are the same as 40 wt% of water system. Also, the strong effect was seen in second coordination shell. The pair correlation function between oxygen atoms in hydronium ion is shown in Figure 24. The shapes of curve are the same for all system and the same position of the first coordination shell in range 4.45 - 4.65 Å which is the same position of second coordination shell between hydronium and water. The coordination number in the first coordination shell is 1.01 in DDA90, while it is 1.19 in DDA80 and 1.13 in DDA70. This shows that the coordination between hydronium ion is weak. The pair correlation function between oxygen atoms in water molecule is shown in Figure 24. There is a strong peak at 2.75 Å, which position have the same opinion with Ennari (2008), 2.8 Å, with coordination number 3.72 in DDA90 and 3.62 in DDA80 and 3.50 in DDA70. This shows that the coordination between water molecules in DDA system, the water clusters are seen. The water clusters can be able to affect to the ion conductivity.

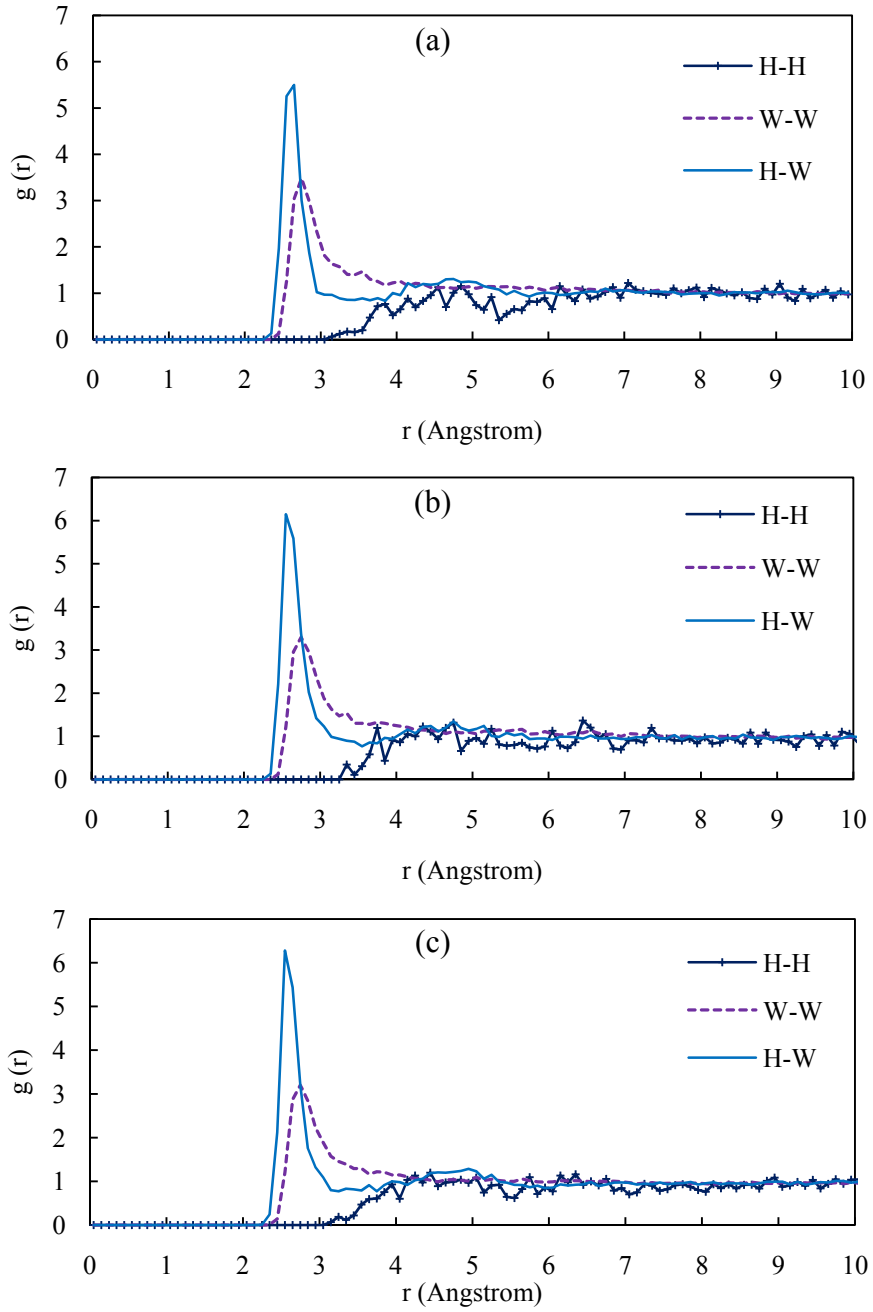

Figure 24 The pair correlation function between the oxygen atom in the hydronium ion and the oxygen atom in water molecule in DDA90 (a), DDA80 (b) and DDA70 (c) system.

In DDA90 system, the pair correlation between the oxygen atom in hidronium ion or water molecule and the nitrogen atom in amino group are shown in Figure 20. The former show the first peak at 2.75 Å with coordination number is 0.57. Pair correlation between the oxygen atom of water and the nitrogen atom of amino group show the first peak at 3.25 Å with coordination number 1.96. Pair correlation function between hydronium or water and hydroxyl group of DDA90 illustrated in Figure 22. The first peak of hydronium ion appeared at 2.55 Å with coordination number 3.55. The pair correlation function between hydronium ion and methoxyl group show the first peak at 3.55 Å with coordination number is 0.5 and between water molecule and methoxyl group are the same, the first peak at 3.55 Å with coordination number is 3.19. The pair correlation function between hydronium ion and acetyl group has a weak peak at 2.95 Å with coordination number is 0.02 and between water molecule and acetyl group illustrates a stronger peak at 2.85 Å with coordination number 1.84. Pair correlation function between the oxygen atom of hydronium ion and the oxygen atom of water molecule show the strong peak at 2.55 Å with the coordination number 3.35 which eigen ion is formed. The pair correlation function between water molecules show a strong peak at 2.75 Å with coordination number 3.72, the water clusters are seen. The water clusters can be seen. This information indicated that the hydronium ions are not mainly located around the functional group of chitosan for 40 % of water.

An amino group ($-NH_2$), nitrogen atom has a lone pair electron, which is high electron density group. The commercial PEM such as Nafion, has a particular group like sulfonic group ($-SO_3^-$) group or PVF-SA and PEO (Ennari *et al*., 2008) the special group is sulfonic group ($-SO_3^-$) which high electron density. The high electron density group can help the transportation of cation by collect the cation around them and transfer the cation to the neighboring group. When the hydrogen of amino group was substituted by the acetyl group ($-COCH_3$) the electron of nitrogen was shared to the acetyl group. Thus, the charge of nitrogen connect to acetyl group is weaker than nitrogen of amino group. When the DDA or amino group per cation decreases that is the reason of the conductivity decrease. This is an idea of transferring mechanism, but the amount of water is important to obtain diffusivity of hydronium ion for hydrated

membrane. The hydronium ions are not mainly located around the functional group of chitosan, but they are elsewhere in water phase. Also eigen ion and water cluster are formed.

The main conclusion can be drawn from the data of Tables 4, 5, 6, 7and 8 is that the coordination number for hydronium ions around the amino group of chitosan is slightly decreased with amount of water. As a conclusion it can be illustrated in Figure 25. This means that the amino group of chain is compensated by the hydronium ion in such a way that the diffusive process may proceed by jumping of the hydronium ion from a fixed group to a neighboring one. The zundle and eigen ion help to transfer the ion through the membrane. However, in the literatures the ion conductivity caused both diffusivity and Grotthus mechanism which to reinforce together. This method simulate the diffusivity of the ions that no creating and breaking bond and no effect of impurity.

The coordination data conclude that functional groups of chitosan have very high water of hydrations, $2H_2O$/amino group, $1H_2O$/hydroxyl group and $3H_2O$/methoxyl group. The amount of water in the system is important to obtain conductivity. Especially, the 40 % of water system eigen ion and water cluster are formed. Water molecule which located around the hydronium ion can be supported the hydronium ion diffuses through the system.

Table 4 Coordination number in the first coordination shell of hydronium-amino and water-amino.

X---Z	System	First coordination shell (Å)	Coordination number, n(1)
H_3O^+---NH_2	Cell1	2.75	0.72
	Cell2	2.75	0.70
	Cell3	2.75	0.48
	Cell4	2.75	0.38
	DDA90	2.75	0.57
	DDA80	2.75	0.36
	DDA70	2.75	0.45
H_2O---NH_2	Cell1	3.05	0.59
	Cell2	3.05	1.10
	Cell3	3.05	1.34
	Cell4	3.05	1.91
	DDA90	3.05	1.96
	DDA80	3.05	1.91
	DDA70	3.05	1.92

Table 5 Coordination number in the first coordination shell of hydronium-hydroxyl and water-hydroxyl

X---Z	System	First coordination shell (Å)	Coordination number, n(1)
H_3O^+---OH	Cell1	2.55	0.72
	Cell2	2.55	0.49
	Cell3	2.55	0.39
	Cell4	2.55	0.28
	DDA90	2.55	0.32
	DDA80	2.55	0.27
	DDA70	2.55	0.28
H_2O---OH	Cell1	2.75	0.70
	Cell2	2.75	1.14
	Cell3	2.75	1.10
	Cell4	2.75	1.48
	DDA90	2.75	1.38
	DDA80	2.75	1.49
	DDA70	2.75	1.32

Table 6 Coordination number in the first coordination shell of hydronium-methoxyl and water-methoxyl.

X---Z	System	First coordination shell (Å)	Coordination number, n(1)
H_3O^+---C	Cell1	3.55	1.17
	Cell2	3.55	0.93
	Cell3	3.55	0.64
	Cell4	3.55	0.48
	DDA90	3.55	0.505
	DDA80	3.55	0.502
	DDA70	3.55	0.55
H_2O---C	Cell1	3.55	1.20
	Cell2	3.55	2.26
	Cell3	3.55	2.66
	Cell4	3.55	3.25
	DDA90	3.55	3.19
	DDA80	3.55	3.36
	DDA70	3.55	3.79

Table 7 Coordination number in the first and second coordination shell of water.

X---Z	System	First coordination shell (Å)	Coordination number, n(1)	Second coordination shell (Å)	Coordination number, n(2)
H_3O^+---	Cell1	2.55	1.06	4.75	1.40
OH_2	Cell2	2.55	1.34	4.75	3.25
	Cell3	2.55	2.63	4.75	5.63
	Cell4	2.55	3.16	4.75	7.04
	DDA90	2.55	3.35	4.75	7.04
	DDA80	2.55	3.22	4.75	6.83
	DDA70	2.55	3.12	4.75	6.72
H_3O^+---	Cell1	4.55	1.69		
OH_3^+	Cell2	4.85	1.41		
	Cell3	4.85	1.22		
	Cell4	4.55	1.09		
	DDA90	4.55	1.01		
	DDA80	4.55	1.19		
	DDA70	4.55	1.13		
H_2O---	Cell1	2.85	0.87		
OH_2	Cell2	2.75	2.02		
	Cell3	2.75	2.92		
	Cell4	2.75	3.58		
	DDA90	2.75	3.72		
	DDA80	2.75	3.62		
	DDA70	2.75	3.50		

Table 8 Coordination number in the first coordination shell between particles X and Y.

X---Z	System	First coordination shell (Å)	Coordination number, n(1)
H_3O^+---O=	DDA90	3.25	0.02
	DDA80	2.85	0.06
	DDA70	2.85	0.39
H_3O^+---N	DDA90	3.35	0.03
	DDA80	3.35	0.36
	DDA70	3.35	0.12
H_2O---O=	DDA90	2.85	1.84
	DDA80	2.85	1.71
	DDA70	2.85	1.89
H_2O---N	DDA90	3.35	1.48
	DDA80	3.35	1.47
	DDA70	3.35	1.58

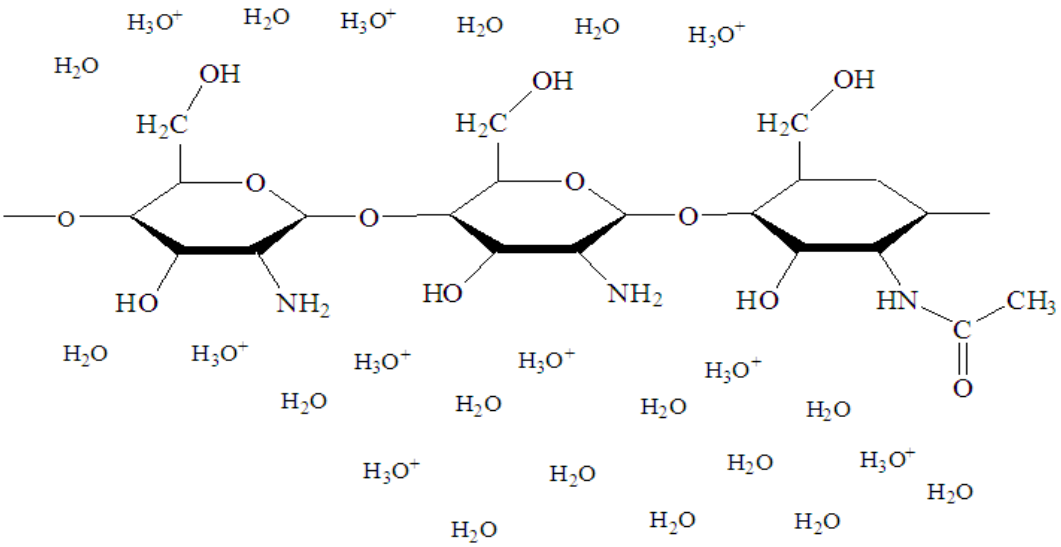

Figure 25 The location of hydronium ions and water molecules around chitosan membrane.

CONCLUSION AND RECOMMENDATION

Conclusion

This work presents the ion conductivity mechanism of chitosan membrane at the molecular level. Firstly, the structure of each particle was constructed and minimized to obtain the stable conformation. Several amorphous systems containing chitosan, hydronium ions and various amounts of water were constructed with periodic boundary condition. Such amorphous systems were simulated by molecular dynamic run. Then, the diffusion coefficient and ion conductivity were calculated from the MSD. The location of the hydronium ion and water molecule were studied by the pair correlation function.

The self-diffusion coefficient can be used to represent the ion conductivity. When the amount of water in the system increased, the diffusivity increased. The 40 wt% of water system was suitable for transferring the ions and followed Arrhenius behavior when temperature increased. The value of conductivity simulated for hydronium ion was in the order of magnitude 10^{-2} S/cm in 40 wt% of water system which was higher than the experimentally found. This was because the hydronium ion could diffuse through the system without creating and breaking bonds. Although there was rather good agreement between simulated and experimental conductivities, more work must be carried out in polyelectrolytes with different chemical structures to assess the reliability of full molecular dynamics to predict ion conductivities of membranes. However, the simulation results did not agree with experimental work when the DDA was varied. This was due to the amount of water making the diffusivity more efficient than the interaction between functional group of chitosan and the ions.

The coordination data illustrate the location of particles in the system. The location of hydronium ion and fixed group of chitosan were concerned. In 40 % of water system hydronium ion are not mainly located around the function group chitosan. While strong coordination between hydronium ions and water molecules increases the ion conductivity. Because the eigen ion and water cluster were important

to obtain conductivity. However, the conductivity was appropriate in the system in which eigen ion and water clusters were formed. The molecular dynamics simulation was used to estimate the diffusion coefficient, the ion conductivity and interactions between particles to get a better understanding of the dynamics behavior of the system.

Recommendation

1. The methodology and technique for improving the conducting polymer are being developed in widespread. Molecular modeling was used to predict the available conducting polymer divided in two branches; Grotthus mechanism and diffusivity of the ion. Both should be used to describe the phenomena in the materials.

2. Recent researches on new materials deal with ion content, water uptake and temperature. Molecular weight is one of the most basic properties of polymer. In the next step, molecular weight would be concerned.

3. Chitosan, a biopolymer, has many advantages such as low cost and environmentally friendly. It has amino groups and hydroxyl groups, which are easily modified to longer side chain or high potential functional groups for development of proton exchange membrane.

4. In the literature of experimental work, considerable efforts have been made to modify the basic structure of chitosan by blending with other materials (Yamada and Honma, 2005, Ramírez-Salgado, 2006). Molecular modeling technique should be used to improve new composite materials.

LITERATURE CITED

Bunte, S. W. and H. Sun. 2000. Molecular modeling of energetic materials: the parameterization and validation of nitrate esters in the COMPASS force field. **Journal of Physical Chemistry B.** 104: 2477-2489.

Devanathan, R., A. Venkatnathan and M. Dupuis. 2007 (a). Structure and Simulation of Nafion Membrane. 1. Effect of hydration on Membrane Nanostructure. **Journal of Physical Chemistry B**. 111: 8069-8079

_____, _____ and _____ 2007 (b). Atomistic Simulation of Nafion Membrane. 2. Dynamics of water Molecules and Hydronium Ions. **Journal of Physical Chemistry B**. 111: 13006-13013

Ennari, J., M. Elomaa and F. Sundholm. 1999. Modeling a polyelectrolyte system in water to estimate the ion-conductivity. **Polymer**. 40: 5035-5041.

_____, I. Neelov and F. Sundholm. 2001. Estimation of the ion conductivity of a PEO-based polyelectrolyte system by molecular modeling. **Polymer.** 42: 8043-8050.

_____. 2008. Modeling of transport properties and state of water of polyelectrolytes containing various amounts of water. **Polymer**. 49: 2373-2380.

Selvan, M.S., J. Lui, D.J. Keffer, S. Cui, B.J. Edwards and W.V. Steele. 2008. Molecular dynamics study of structure and transport of water and hydronium ions at the membrane/vapor interface of Nafion. **Journal of Physical Chemistry C.** 112: 1975-1984.

Hehre, W.J., L. Radom, P.V.R. Schleyer and J.A. Pople. 1986. **Ab initio Molecular Orbital Theory.** 1st ed. JohnWiley & Sons, Inc., Canada.

Hickner, M.A., H. Ghassemi, Y.S. Kim, B.R. Einsla, and J.E. McGrath. 2004. Alternative polymer systems for proton exchange membranes (PEMs). **Chemical Reviews**. 104: 4587- 4612.

Kim, E., P. F. Weck, N. Balakrishnan and C. Bae. 2008. Nanoscale building blocks for the development of novel proton exchange membrane Fuel Cells. **Journal of Physical Chemistry B**. 112: 3283-3286

Kreuer, K.D. 2000. On the complexity of proton conduction phenomena. **Solid State Ionics**. 136–137: 149–160

_____, S.J. Paddison, E. Spohr and M. Schusterv. 2004. Transport in Proton Conductors for Fuel-Cell Applications: Simulations, Elementary Reactions, and Phenomenology. **Chemical Reviews**. 104: 4637-4678.

Leach, A.R. 1996. **Molecular Modelling Principles and Applications.** 2nd ed. Addison Wesley Longman Ltd., Harlow Essex, England.

López-Chávez, E., J.M. Martínez-magadán, R. Oviedo-Roa, J. Guzmán, J. Ramírez-Salgado and J. Marín-Cruz. 2005. Molecular modeling and simulation of ion-conductivity in chitosan membranes. **Polymer**. 46: 7519-7527.

Mukoma, P., B.R. Jooste and H.C.M. Vosloo. 2004. Synthesis and characterization of cross-linked chitosan membranes for application as alternative proton exchange membrane materials in fuel cells. **Journal of Power Sources.** 136: 16-23.

Paddison, S.J., and J.A. Elliott. 2007. Selective hydration of the 'short-side-chain' perfluorosulfonic acid membrane. An ONIOM study. **Solid State Ionics**. 178: 561–567.

Pozuelo, J., E. Riande, E. Saiz and V. Compañ. 2006. Molecular dynamics simulations of proton conduction in Sulfonated poly(phenyl sulfone)s. **Macromolecules**. 39: 8862-8866.

Punnasukhirom, V. 2006. **Investigation on Structural and Energetic Properties of Chitosan Membrane Surface of PEM Fuel Cell by Quantum Chemical Calculations**. M.Eng. Thesis, Kasetsart University

Ramiez, P., S. Mafe, A. Tanioka and K. Saito. 1997. Modeling of membrane potential and ionic flux in weak amphoteric polymer membranes. **Polymer.** 38: 4931-4934

Ramírez-Salagado, J. 2007. Study of basic biopolymer as proton membrane for fuel cell systems. **Elecreochemica Acta**. 52: 3766-3778.

Ravi Kumar, M.N.V. 2000. A review of chitin and chitosan applications. **Reactive and Functional Polymers.** 46: 1 –27

Sun, H. 1998. COMPASS: An ab initio force-field optimized condensed-phase applications overview with details on alkane and benzene compounds. **Journal of Physical Chemistry B.** 102: 7338-7364.

Venkatnathan, A., R. Devanathan, and M. Dupuis. 2007 (a). Atomistic Simulation of Hydrated Nafion and Temperature Effects on Hydronium Ion Mobility. **Journal of Physical Chemistry B**. 111: 7234-7244

Wan, Y., K. A.M. Creber, B. Peppley and V. Tam Bui. 2003. Ionic conductivity of chitosan Membranes. **Polymer.** 44: 1057-1065.

Yamada, M. and I. Honma. 2005. Anhydrous proton conductive membrane consisting of chitosan. **Electrochemica Acta**. 50: 2837-2841.

Yang, J., Y. Ren, A. Tian and H. Sun. COMPASS force field for 14 inorganic molecules, He, Ne, Ar, Kr, Xe, H2, O2, N2, NO, CO, CO2, NO2, CS2, and SO2, in liquid phases. **Journal of Physical Chemistry B.** 104: 24951-4957.

APPENDICES

Appendix A

Molecular structure of Chitosan

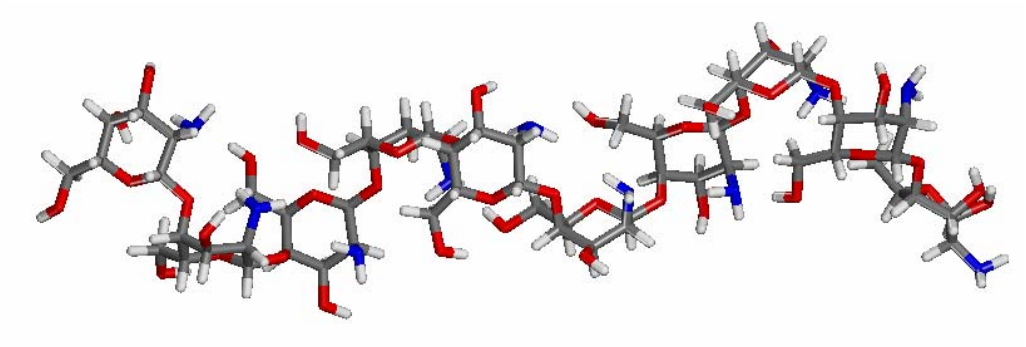

Appendix Figure A1 Molecular structure of chitosan.

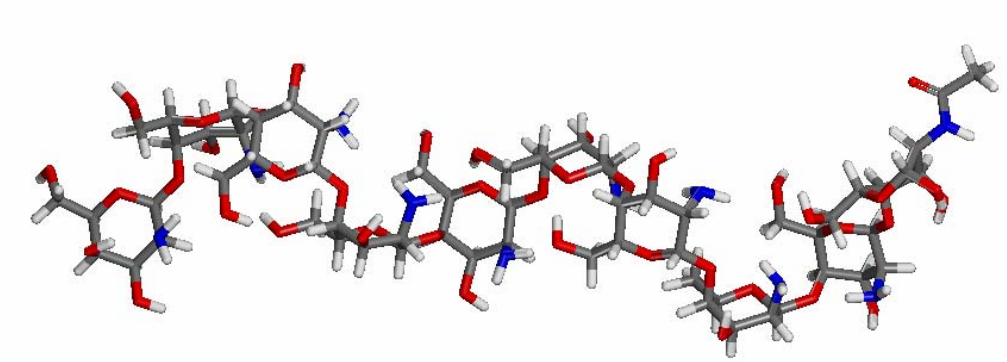

Appendix Figure A2 Molecular structure of 90% DDA chitosan.

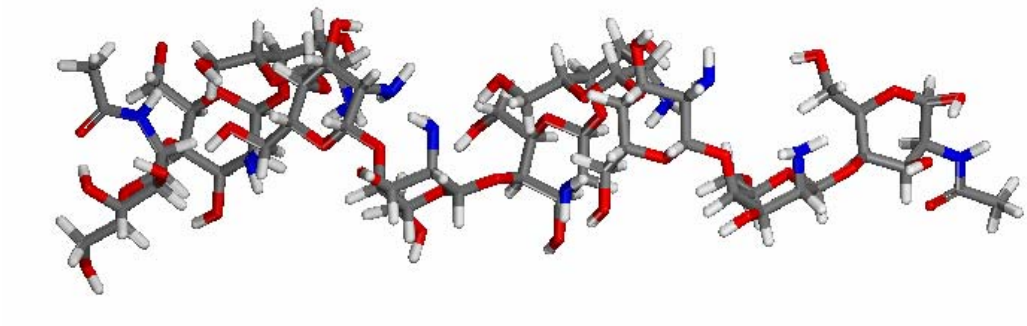

Appendix Figure A3 Molecular structure of 80% DDA chitosan.

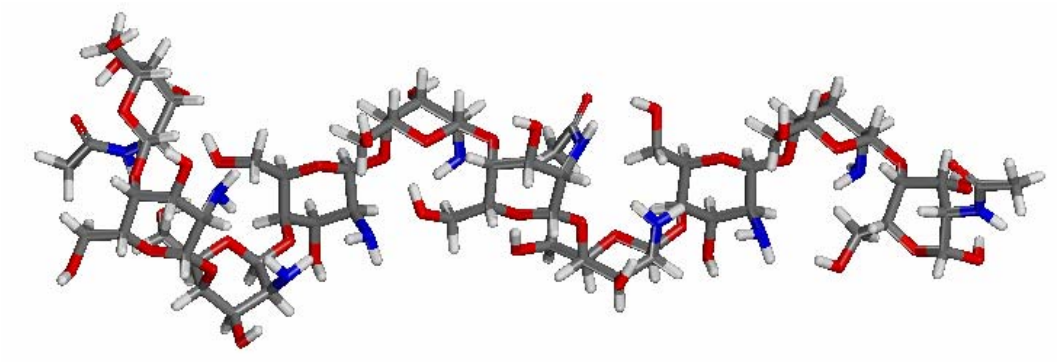

Appendix Figure A4 Molecular structure of 70% DDA chitosan.

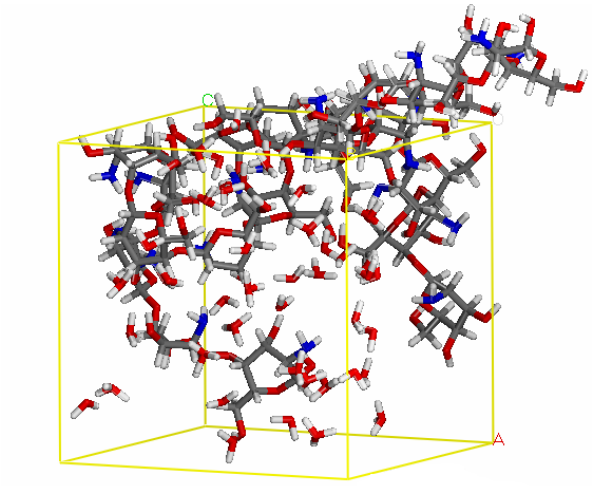

Appendix Figure A5 Amorphous system for cell1 (10% water).

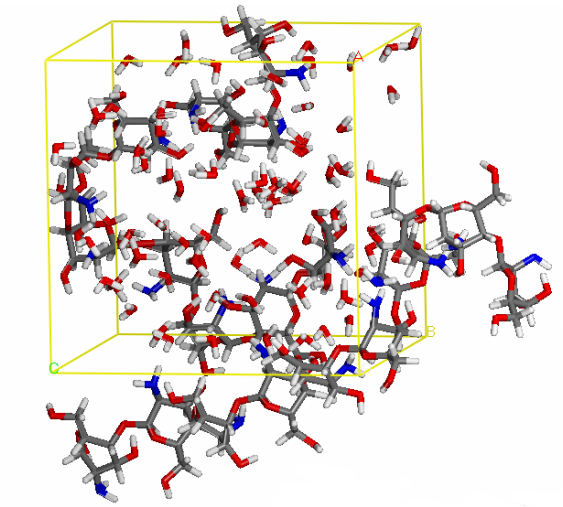

Appendix Figure A6 Amorphous system for cell2 (20% water).

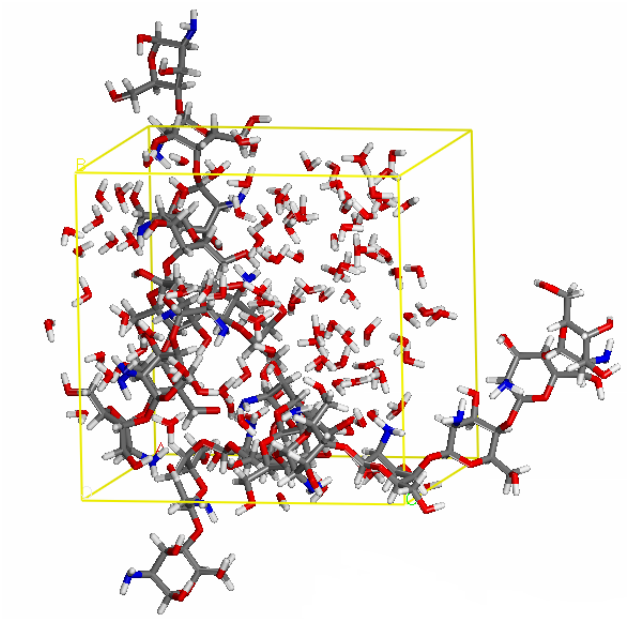

Appendix Figure A7 Amorphous system for cell3 (30% water).

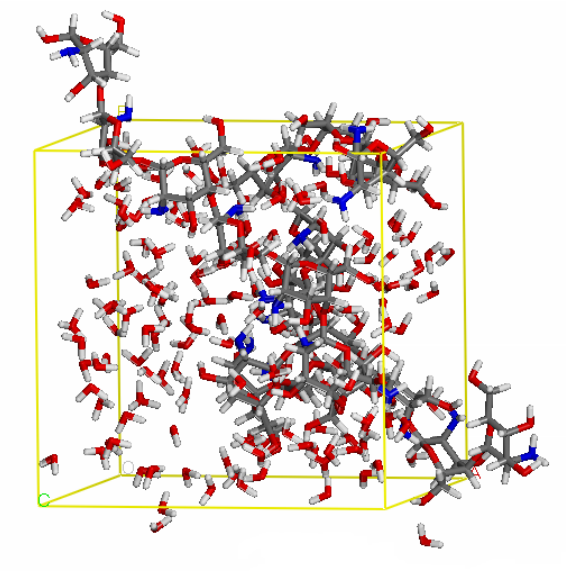

Appendix Figure A8 Amorphous system for cell4 (40% water).

Appendix B

Dynamical results and calculations

Appendix Table B1 Mean square displacement.

298 K	MSD ($Å^2$)			
Time (ps)	Cell1	Cell2	Cell3	Cell4
5	0.71905	0.77288	1.2965	1.8351
10	0.99342	1.0236	2.0259	2.9947
15	1.1898	1.2509	2.7155	4.097
20	1.3532	1.5205	3.3948	5.1162
25	1.507	1.794	3.9989	6.0304
30	1.676	2.0489	4.4915	6.8406
35	1.8225	2.2704	4.9823	7.6345
40	1.9308	2.4341	5.412	8.4218
45	2.0514	2.7213	5.8911	9.1818
50	2.0499	2.9193	6.5201	9.877
55	2.1794	3.1738	7.1864	10.656
60	2.2734	3.3833	7.6641	11.302
65	2.347	3.5525	8.1122	12.059
70	2.4691	3.8026	8.6894	12.784
75	2.5788	3.9733	9.2999	13.491
80	2.6692	4.1713	9.8599	14.391
85	2.7729	4.3726	10.49	15.092
90	2.8842	4.6154	11.191	15.845
95	3.0494	4.8332	11.995	16.646
100	3.1188	5.0309	12.616	17.699
105	3.302	5.2674	13.415	18.652
110	3.5414	5.5346	14.007	19.285
115	3.7482	5.7101	14.56	20.127
120	3.9324	5.9481	15.095	20.771
125	4.1172	6.054	15.534	21.269
130	4.3718	6.0891	15.95	22.01
135	4.6893	6.051	16.187	22.719

Appendix Table B1 (Continued)

298 K	MSD ($Å^2$)			
Time (ps)	Cell1	Cell2	Cell3	Cell4
140	4.9463	5.9104	16.437	23.655
145	5.1774	5.9691	16.954	24.759
150	5.496	6.1931	17.411	25.762
155	5.8261	6.358	18.071	27.057
160	6.1753	6.612	18.595	29.168
165	6.3665	6.5612	18.931	31.275
170	6.6766	6.8967	19.223	33.357
175	6.97	7.2621	19.694	35.616
180	7.2806	7.5986	20.59	37.198
185	7.3499	7.6589	22.042	38.508
190	7.3223	7.6082	22.773	40.529
195	7.5922	7.577	26.233	41.085

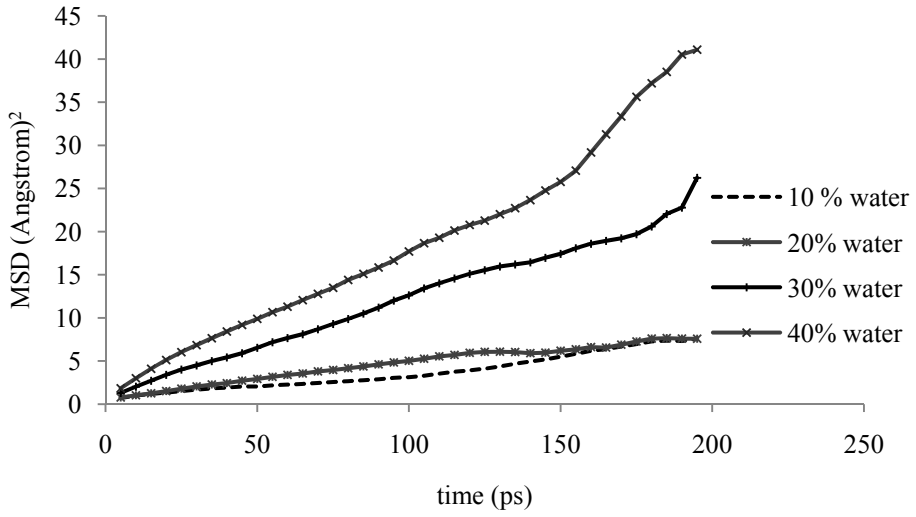

Appendix Figure B1 Mean square displacement of hydronium ion as a function of time at 298 K.

Example: Cell4

Slope of this curve = 0.192 $Å^2$/ps

The diffusivity is given by

$$D_\alpha = \frac{1}{6N_\alpha} \lim_{t\to\infty} \frac{d}{dt} \sum_{i=1}^{N_\alpha} \langle [R_i(t) - R_i(0)]^2 \rangle \tag{4}$$

$$D = \text{slope}/6 = 0.032 \times 10^{-8}\ m^2/s$$

Where

$V = 7752.987\ Å^3$

$k = 8.617 \times 10^{-5}$ eV/K

$e = 1.02 \times 10^{-19}$

z = 1

T = 298 K

N = 20

$$\sigma = \frac{Nz^2e^2D}{VkT} \tag{5}$$

$$\sigma = 0.0714\ S/cm$$

Appendix C

Coordination results and coordination number calculations

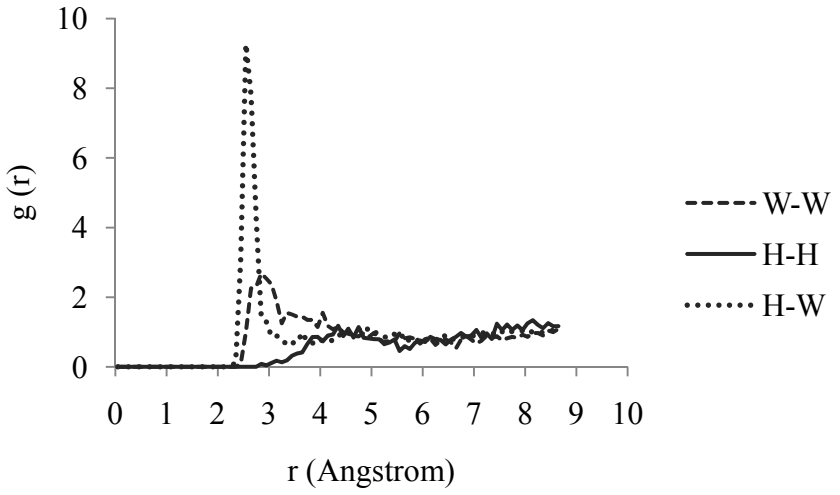

Appendix Figure C1 The pair correlation function between the oxygen atom in the hydronium ion and the oxygen atom in water molecule in Cell1.

Appendix Table C1 Pair correlation function between H_3O^+---H_2O and coordination number calculation in Cell1.

r (Å)	r^2	dr	g (r)	$4\pi\rho g(r)r^2dr$
2.15	4.6225	0.1	0	0
2.25	5.0625	0.1	0.029478	0.000833
2.35	5.5225	0.1	0.10809	0.003331
2.45	6.0025	0.1	3.1326	0.104932
2.55	6.5025	0.1	9.272	0.336452
2.65	7.0225	0.1	7.8205	0.306476
2.75	7.5625	0.1	4.2823	0.180722
2.85	8.1225	0.1	1.4148	0.064129
2.95	8.7025	0.1	1.2862	0.062463
	Coordination number, n = $\Sigma\ 4\pi\rho g(r)r^2dr$		=	1.059

ρ = N/V N = 23 molecules of H_2O V = 5176.64 $Å^3$

Appendix Table C2 Pair correlation function between H_3O^+---H_2O and coordination number calculation in Cell2.

r (Å)	r^2	dr	g (r)	$4\pi\rho g(r)r^2dr$
2.25	5.0625	0.1	0	0
2.35	5.5225	0.1	0.10794	0.006662
2.45	6.0025	0.1	2.9793	0.199873
2.55	6.5025	0.1	8.2621	0.600452
2.65	7.0225	0.1	6.9819	0.54799
2.75	7.5625	0.1	3.7147	0.313976
2.85	8.1225	0.1	1.7706	0.160738
2.95	8.7025	0.1	1.156	0.112437
	Coordination number, n = $\Sigma\, 4\pi\rho g(r)r^2dr$ =			1.342

N = 52 molecules of H_2O V = 5843.672 $Å^3$

Appendix Table C3 Pair correlation function between H_3O^+---H_2O and coordination number calculation in Cell3.

r (Å)	r^2	dr	g (r)	$4\pi\rho g(r)r^2dr$
2.15	4.6225	0.1	0	0
2.25	5.0625	0.1	0	0
2.35	5.5225	0.1	0.1882	0.017489
2.45	6.0025	0.1	2.4324	0.245678
2.55	6.5025	0.1	7.1471	0.782005
2.65	7.0225	0.1	6.1528	0.727049
2.75	7.5625	0.1	3.3443	0.425569
2.85	8.1225	0.1	1.6879	0.230694
2.95	8.7025	0.1	1.3934	0.204042
	Coordination number, n = $\Sigma\, 4\pi\rho g(r)r^2dr$ =			2.632

N = 90 V = 6717.889 $Å^3$

Appendix Table C4 Pair correlation function between H_3O^+---H_2O and coordination number calculation in Cell4.

r (Å)	r^2	dr	g (r)	$4\pi\rho g(r)r^2dr$
2.15	4.6225	0.1	0	0
2.25	5.0625	0.1	0	0
2.35	5.5225	0.1	0.031028	0.003748
2.45	6.0025	0.1	1.9698	0.258588
2.55	6.5025	0.1	6.2367	0.88693
2.65	7.0225	0.1	5.8319	0.895687
2.75	7.5625	0.1	3.278	0.542162
2.85	8.1225	0.1	1.8354	0.326043
2.95	8.7025	0.1	1.3259	0.252353
	Coordination number, n = $\Sigma\ 4\pi\rho g(r)r^2dr$		=	3.165

N = 135 molecules of H_2O V = 7752.987 $Å^3$

Appendix Table C5 Pair correlation function between H_3O^+---H_2O and coordination number calculation in DDA90.

r (Å)	r^2	dr	g (r)	$4\pi\rho g(r)r^2dr$
2.15	4.6225	0.1	0	0
2.25	5.0625	0.1	0	0
2.35	5.5225	0.1	0.13246	0.01599
2.45	6.0025	0.1	1.9651	0.257837
2.55	6.5025	0.1	5.2521	0.74652
2.65	7.0225	0.1	5.4948	0.843474
2.75	7.5625	0.1	3.0047	0.4967
2.85	8.1225	0.1	1.8688	0.331803
2.95	8.7025	0.1	1.0245	0.194887
	Coordination number, n = $\Sigma\ 4\pi\rho g(r)r^2dr$		=	2.887

N = 138 molecules of H_2O V = 7929.409 $Å^3$

Appendix Table C6 Pair correlation function between H_3O^+---H_2O and coordination number calculation in DDA80.

r (Å)	r^2	dr	g (r)	$4\pi\rho g(r)r^2dr$
2.15	4.6225	0.1	0	0
2.25	5.0625	0.1	0	0
2.35	5.5225	0.1	0.13252	0.015989
2.45	6.0025	0.1	2.2099	0.289812
2.55	6.5025	0.1	6.1481	0.87344
2.65	7.0225	0.1	5.5887	0.857461
2.75	7.5625	0.1	3.3751	0.557653
2.85	8.1225	0.1	2.0274	0.359783
2.95	8.7025	0.1	1.4192	0.269836
	Coordination number, n = $\Sigma\, 4\pi\rho g(r)r^2dr$		=	3.224

N = 141 molecules of H_2O V = 8105.823 $Å^3$

Appendix Table C7 Pair correlation function between H_3O^+---H_2O and coordination number calculation in DDA70.

r (Å)	r^2	dr	g (r)	$4\pi\rho g(r)r^2dr$
2.15	4.6225	0.1	0	0
2.25	5.0625	0.1	0.009039	0.000999
2.35	5.5225	0.1	0.24031	0.028981
2.45	6.0025	0.1	2.1194	0.277815
2.55	6.5025	0.1	6.2777	0.891437
2.65	7.0225	0.1	5.4349	0.833476
2.75	7.5625	0.1	3.2072	0.529665
2.85	8.1225	0.1	1.7579	0.311813
2.95	8.7025	0.1	1.32	0.250858
	Coordination number, n = $\Sigma\, 4\pi\rho g(r)r^2dr$		=	3.125

N = 144 molecules of H_2O V = 8282.133 $Å^3$

CURRICULUM VIATE

NAME : Ms. Suwalee Martkumchan

BIRTH DATE : November 5, 1984

BIRTH PLACE : Prachin Buri, Thailand

EDUCATION :

YEAR	**INSTITUTION**	**DEGREE/DIPLOMA**
2003-2007	Kasetsart University	B. S. (Chemistry)